

# Spin dynamics in finite cyclic $XY$ model

Evgeniy Safonov <sup>a</sup>, Oleg Lychkovskiy <sup>b,a</sup>

<sup>a</sup> *Institute for Theoretical and Experimental Physics*

*117218, B.Chermushkinskaya 25, Moscow, Russia*

<sup>b</sup> *Physics Department, Lancaster University, Lancaster, LA1 4YB, UK*

## Abstract

Evolution of the  $z$ -component of a single spin in the finite cyclic  $XY$  spin  $1/2$  chain is studied. Initially one selected spin is polarized while other spins are completely unpolarized and uncorrelated. Polarization of the selected spin as a function of time is proportional to the autocorrelation function  $g_0^{zz}(t)$  at infinite temperature. The initial perturbation gives rise to two wave packets moving in opposite directions and winding over the circle. We express  $g_0^{zz}(t)$  as a series in winding number and derive tractable approximations for each term. This allows to give qualitative explanation and quantitative description to various finite-size effects such as partial revivals and regular-to-chaotic transition.

## Contents

<b>1</b>	<b>Introduction</b>	<b>2</b>
<b>2</b>	<b><math>XY</math> model on a circle</b>	<b>4</b>
<b>3</b>	<b>Reduced dynamics of a spin at <math>T = \infty</math></b>	<b>4</b>
3.1	Correlation function: sum over modes . . . . .	4
3.2	Correlation function: sum over winding numbers . . . . .	6
3.3	Special case: $XX$ chain . . . . .	7
3.4	Special case: Ising chain with $h = 1$ . . . . .	8
<b>4</b>	<b>Asymptotic approximations</b>	<b>8</b>
4.1	Winding of a wave packet over a circle . . . . .	8
4.2	Asymptotic approximations for $t < t_{\text{th}}$ . . . . .	11
4.3	Asymptotic approximations for $t > jt_{\text{th}}$ . . . . .	13
4.4	Partial revivals . . . . .	14
<b>5</b>	<b>Transition from regular to chaotic evolution</b>	<b>15</b>
<b>6</b>	<b>Discussion and conclusions</b>	<b>17</b>

<b>A</b>	<b>Diagonalization of finite cyclic <math>XY</math> spin chain</b>	<b>18</b>
A.1	Ranges of parameters . . . . .	18
A.2	$H$ in terms of $\sigma_n^\pm$ . . . . .	19
A.3	Jordan-Wigner transformation . . . . .	20
A.4	Fourier transformation . . . . .	20
A.5	Bogolyubov transformation . . . . .	21
A.6	Eigenstates . . . . .	22
<b>B</b>	<b>Calculation of <math>g_n^{zz}(t)</math></b>	<b>23</b>
<b>C</b>	<b>Group velocity of spin waves</b>	<b>24</b>
<b>D</b>	<b>Asymptotic expressions</b>	<b>26</b>
D.1	Asymptotics for spectral functions of zero order . . . . .	27
D.2	Asymptotics for spectral functions of non-zero order . . . . .	29
D.2.1	Asymptotics for $t > jt_{\text{th}}$ . . . . .	30
D.2.2	Asymptotics for $t < jt_{\text{th}}$ . . . . .	32
D.2.3	Asymptotics for $t \simeq jt_{\text{th}}$ . . . . .	34

# 1 Introduction

Exactly solvable spin chains are widely used as toy models for exploring various aspects of quantum dynamics. Recent progress in experimental techniques allows to construct quantum systems with effective spin chain Hamiltonians (see e.g. [1]), which opens new prospects for exploring fundamental concepts such as thermalization and emergence of chaos, as well as for applications such as quantum state transfer through quantum wires [2]. This motivates further efforts to understand dynamics of spin chains in detail.

We consider the reduced dynamics of a single spin in the cyclic spin  $1/2$   $XY$  chain with finite number of spins,  $N$ . Initially one selected spin has a given polarization while other  $(N - 1)$  spins are completely uncorrelated and unpolarized. We study the  $z$ -component of polarization of a spin as a function of time. It can be expressed through the two-spin time-dependent correlation functions  $g_n^{zz}(t)$ . Although many papers starting from the pioneering paper on  $XY$  chain [3] were devoted to calculation of various correlation functions, most of the studies concentrated on the thermodynamic limit  $N \rightarrow \infty$ . Exact expression for  $g_n^{zz}(t)$  in the  $XY$  model with finite  $N$  was derived in [4, 5]. It involves sums of  $\sim N$  oscillating terms and thus is not easily tractable. However, it allows to plot  $g_n^{zz}(t)$  for various values of model parameters. Such plots readily reveal a rich variety of spin evolution patterns which call for explanation (see figures in the present paper, especially fig. 1). One striking feature of the evolution is regular-to-chaotic transition:  $g_n^{zz}(t)$  is described fairly well by  $N \rightarrow \infty$  approximation (which is given by a rather regular function of time for a wide range of model parameters) up to some threshold time  $t_{\text{th}}$ , but at  $t_{\text{th}}$  this concordance is abruptly destroyed by sharp revival; at later times the evolution becomes less and less regular and ends up with apparently chaotic fluctuations near the long-time average. This feature is common for all finite spin chains; in particular, it was

observed in the  $XX$  (isotropic  $XY$ ) model [6, 7], in the  $XXZ$  model with long-range [8] and nearest-neighbor [9] couplings, in the  $XY$  model [10].

What underlies the regular-to-chaotic transition in the cyclic chain is the winding of two oppositely directed wave packets created by the initial perturbation [7] (or reflection from the ends of the chain in case of linear chain [6]). Threshold time corresponds to the time necessary for the forefronts of the wave packets to make one round trip over the circle. The interference between the forefronts of the wave packets and their own tails produces partial revivals at  $t = t_{\text{th}}, 2t_{\text{th}}, \dots$  and leads to the regular-to-chaotic transition.

In order to study spin dynamics in finite spin chains at times greater than  $t_{\text{th}}$  it is desirable to have tractable approximate expressions for  $g_n^{zz}(t)$  valid for  $t > t_{\text{th}}$ . The goal of the present paper is to obtain such approximations for the cyclic  $XY$  model. The mathematical method which we introduce is closely related to the physical picture of wave packet winding over the circle and in fact allows to quantitatively describe such winding. A winding number  $s$  given, we are able to get the approximate expression which is valid up to  $(s + 1)t_{\text{th}}$  and describes interference between the components of the wave packets which have completed  $0, 1, 2, \dots, s$  round trips over the circle. These approximations are fairly accurate even when the evolution is already apparently chaotic. A related result was obtained in [11] in a special case of  $XX$  model: they represent Green function of a quasi-particle through a sum over winding numbers.

The obtained approximate expressions involve  $\sim s$  oscillating terms and therefore are much more tractable than the exact formula as long as  $s \ll N$ . They allow to look at the regular-to-chaotic transition (as well as on some other peculiar features of spin evolution in finite chains) from a new perspective. However in the present paper we only briefly discuss this issue postponing more extended study for future work.

We also touch the issue of incomplete thermalization of spins in the  $XY$  spin chain. In particular we show that the autocorrelation function  $g_0^{zz}(t)$  at infinite temperature never changes its sign in contrast to what should be expected in case of complete thermalization. This intriguing property was previously proven in the special case of the  $XX$  chain [6, 7] and observed in numerical calculations of spin evolution in the  $XXZ$  model with long-range interactions [8].

The rest of the paper is organized as follows. In Sec. 2 we briefly describe the  $XY$  model on a circle. In Sec. 3 we discuss exact formula for  $g_n^{zz}(t)$  and rewrite it in a form suitable for subsequent analysis. In two special cases (one of them is the  $XX$  model) we represent  $g_n^{zz}(t)$  in transparent and convenient way through the infinite sum of Bessel functions; such representation allows to obtain simple successive approximations valid up to times  $t_{\text{th}}, 2t_{\text{th}}, \dots$ . In Sec. 4 we present our main result – the successive asymptotic approximations in a general case. In Sec. 5 we discuss the emergence of chaos in the course of spin evolution. The results are summarized in Sec. 6. Bulk of technical details is presented in Appendices. In Appendix A we describe the diagonalization of the  $XY$  model. In Appendix B we rederive the exact formula for  $g_n^{zz}(t)$  at infinite temperature using a method which is somewhat more direct than one implemented in the original work [4, 5]. These two appendices mostly contain widely known calculations and results; however we include them in order to introduce our notations, to emphasize some salient features usually omitted in the literature and for the sake of completeness. In Appendix C the dependance of the wave packet forefront velocity on the model parameters is inves-

tigated. Appendix D contains the technical details of calculating asymptotic expressions presented in Sec. 4.

## 2 XY model on a circle

We consider a chain of  $N$  coupled spins  $1/2$  with the following Hamiltonian [3, 12]:

$$H = \frac{1}{4} \sum_{n=1}^N ((1 + \gamma) \sigma_n^x \sigma_{n+1}^x + (1 - \gamma) \sigma_n^y \sigma_{n+1}^y) + \frac{h}{2} \sum_{n=1}^N \sigma_n^z. \quad (1)$$

Here the index  $N + 1$  is identified with 1, and  $N$  is supposed to be even. Two parameters enter the Hamiltonian, the anisotropy parameter  $\gamma$  and the magnetic field  $h$ . Without loss of generality one may assume  $\gamma \geq 0$ ,  $h \geq 0$  (see Appendix A). In Sec. 4 we will concentrate on the case  $h \geq 1$ ,  $\gamma \in [0, 1]$ .

Finite XY model is "almost diagonalizable" through the sequential Jordan-Wigner, Fourier and Bogolyubov transformations [3, 4, 5]. The details of the XY spin chain diagonalization are presented in the appendix A.

An important property of the XY Hamiltonian is that it commutes with the parity operator  $\Pi \equiv \prod_{n=1}^N \sigma_n^z$ . The diagonalization leads to the "almost free fermion form" of the Hamiltonian:

$$H = P^{\text{odd}} \sum_{q \in X_{\text{odd}}} E_q (c_q^+ c_q - \frac{1}{2}) + P^{\text{ev}} \sum_{q \in X_{\text{ev}}} E_q (c_q^+ c_q - \frac{1}{2}), \quad (2)$$

where

$$X_{\text{odd}} = \{-\frac{N}{2} + 1, -\frac{N}{2} + 2, \dots, \frac{N}{2}\}, \quad X_{\text{ev}} = \{-\frac{N}{2} + \frac{1}{2}, -\frac{N}{2} + \frac{3}{2}, \dots, \frac{N}{2} - \frac{1}{2}\}, \quad (3)$$

$\{c_q, q \in X_{\text{odd}}\}$  and  $\{c_q, q \in X_{\text{ev}}\}$  are two sets of fermion operators (note, however, that two operators from different sets do not satisfy fermion anticommutation relations, see eq.(A-21)),  $P^{\text{odd}}$  and  $P^{\text{ev}}$  are parity projectors,

$$P^{\text{ev}} \equiv (1 + \Pi)/2, \quad P^{\text{odd}} \equiv (1 - \Pi)/2, \quad (4)$$

and fermion energy is defined as  $E_q \equiv E(\varphi(q))$ ,  $\varphi(q) \equiv \frac{2\pi q}{N}$ ,

$$E(\varphi) = \sqrt{\varepsilon(\varphi)^2 + \Gamma(\varphi)^2}, \quad \varepsilon(\varphi) \equiv h - \cos \varphi, \quad \Gamma(\varphi) \equiv \gamma \sin \varphi. \quad (5)$$

One can see that the Hilbert space is divided into a two subspaces with odd and even numbers of fermions correspondingly. Number of fermions is an integral of motion, and when it is fixed, the model looks like a free-fermion model.

## 3 Reduced dynamics of a spin at $T = \infty$

### 3.1 Correlation function: sum over modes

We focus our study on the  $z$ -component of the  $n$ 'th spin polarization vector as a function of time:

$$p_n^z(t) \equiv \text{tr}[\rho(t) \sigma_n^z], \quad (6)$$

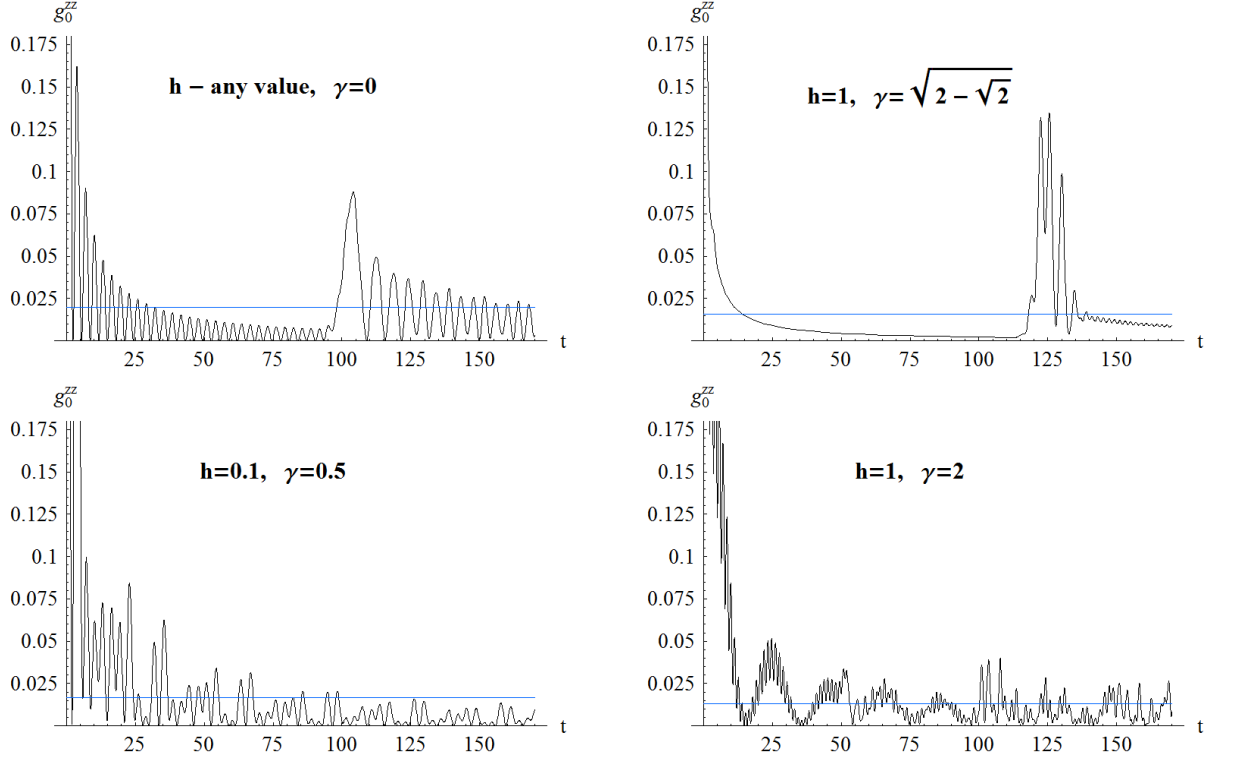


Figure 1: Patterns of spin dynamics for various values of model parameters. Exact auto-correlation function  $g_0^{zz}(t)$  is plotted. According to eq. (9) it is equal to the polarization of the first spin  $p_1^z(t)$  provided  $p_1^z(0) = 1$ . Horizontal line (blue online) marks the long-time average of the autocorrelation function given by eq.(B-10). Number of spins here and in all other plots in the paper is  $N = 100$ .

where  $\rho(t) = e^{-iHt}\rho(0)e^{iHt}$  is the density matrix of the whole chain.

We choose the following initial condition:

$$\rho(0) = 2^{-N}(\mathbb{1}_1 + \mathbf{p}_1(0)\boldsymbol{\sigma}_1) \otimes \mathbb{1}_{23\dots N}. \quad (7)$$

It describes a situation when at  $t = 0$  the first spin has an arbitrary polarization  $\mathbf{p}_1(0)$ , while other  $(N - 1)$  spins are completely unpolarized and uncorrelated. If the first spin is regarded as an open system, while other  $(N - 1)$  spins – as an environment, then such initial condition corresponds to infinite temperature of the environment. Given the above initial condition, the polarization  $p_n^z(t)$  can be expressed through the two-spin correlation functions at infinite temperature,  $p_n^z(t) = p_1^\alpha(0)g_{n-1}^{z\alpha}(t)$ , where

$$g_n^{z\alpha}(t) \equiv 2^{-N}\text{tr}[\sigma_{n+1}^\alpha(t)\sigma_1^z]. \quad (8)$$

Due to conservation of parity  $g_n^{zx}(t) = g_n^{zy}(t) = 0$  and we are left with

$$p_n^z(t) = p_1^z(0)g_{n-1}^{zz}(t). \quad (9)$$

Note that such relation between the polarization of a single spin and the correlation function holds only in the case of infinite temperature.

Thus our problem reduces to investigation of the  $zz$  correlation function. Due to integrability of the model it may be calculated exactly [4, 5]. For the completeness of the presentation we provide the details of calculation in Appendix B. The result reads:

$$g_n^{zz}(t) = \frac{1}{2}(A_{\text{odd}}^n{}^2 + A_{\text{ev}}^n{}^2 + B_{\text{odd}}^n{}^2 + B_{\text{ev}}^n{}^2 - C_{\text{odd}}^n{}^2 - C_{\text{ev}}^n{}^2), \quad (10)$$

where

$$\begin{aligned} A_{\text{ev(odd)}}^n(t) &= N^{-1} \sum_{q \in X_{\text{ev(odd)}}} \cos n\varphi(q) \cos E_q t, \\ B_{\text{ev(odd)}}^n(t) &= N^{-1} \sum_{q \in X_{\text{ev(odd)}}} \frac{\varepsilon_q}{E_q} \cos n\varphi(q) \sin E_q t, \\ C_{\text{ev(odd)}}^n(t) &= N^{-1} \sum_{q \in X_{\text{ev(odd)}}} \frac{\Gamma_q}{E_q} \sin n\varphi(q) \sin E_q t. \end{aligned} \quad (11)$$

In what follows we mainly concentrate on the evolution of the first spin which is distinguished by the initial condition. It is described by the autocorrelation function  $g_0^{zz}(t)$ .

As was noticed in [7], in case of the  $XX$  model ( $\gamma = 0$ )  $g_n^{zz}(t)$  is always non-negative (because  $C_{\text{ev(odd)}}^n(t) = 0$ ) or, in other words, spin polarization never changes its sign. We see that this is not the case for an arbitrary site  $n$  in a general  $XY$  chain. However, the polarization of the first spin still never changes its sign since  $C_{\text{ev(odd)}}^0(t) = 0$  for any  $\gamma$ . Intriguingly, the same property (non-negativity of  $g_0^{zz}(t)$  at infinite temperature) was observed in numerical simulations for the  $XXZ$  model with long-range interactions [8]. This suggests that this effect could be generic for a large class of spin systems.

Surprisingly enough, evolution of spin polarization described by the exact formula (10) exhibits a rich variety of patterns depending on  $h$  and  $\gamma$ . Examples are given in Fig. 1. We aim at explaining major features of evolution and at providing tractable approximation to eq.(10).

### 3.2 Correlation function: sum over winding numbers

Let us rewrite formulae (11) for  $n = 0$  in a different form:

$$\begin{aligned} A_{\text{odd}}^0(t) &= A_0(t) + 2 \sum_{j=1}^{\infty} A_j(t), & A_{\text{ev}}^0(t) &= A_0(t) + 2 \sum_{j=1}^{\infty} (-1)^j A_j(t), \\ B_{\text{odd}}^0(t) &= B_0(t) + 2 \sum_{j=1}^{\infty} B_j(t), & B_{\text{ev}}^0(t) &= B_0(t) + 2 \sum_{j=1}^{\infty} (-1)^j B_j(t), \end{aligned} \quad (12)$$

where

$$\begin{aligned} A_j(t) &\equiv (2\pi)^{-1} \text{Re} \int_{-\pi}^{\pi} e^{i(E(\varphi)t - jN\varphi)} d\varphi, \\ B_j(t) &\equiv (2\pi)^{-1} \text{Im} \int_{-\pi}^{\pi} \frac{\varepsilon(\varphi)}{E(\varphi)} e^{i(E(\varphi)t - jN\varphi)} d\varphi. \end{aligned} \quad (13)$$

As will be shown below  $j$  corresponds to a number of windings of a forefront of a wave packet produced by the initial perturbation. To obtain the above expressions one should

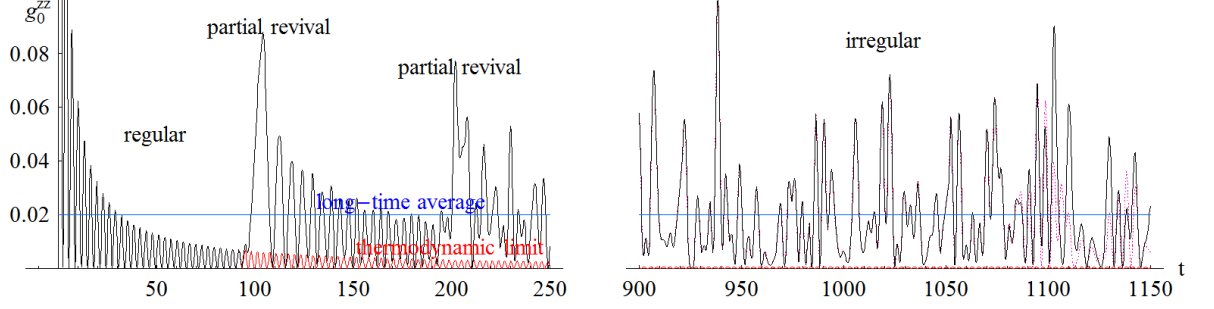


Figure 2:  $g_0^{zz}(t)$  for the  $XX$  model. Threshold time is  $t_{\text{th}} = 100$ . Solid line corresponds to the exact expression. Dotted line (magenta online) corresponds to the approximation (17) with  $j = 0, 1, \dots, 10$ . One can see that the approximation starts to deviate from the exact expression only at  $t \simeq 11t_{\text{th}}$ . Approximation obtained in thermodynamic limit ( $j = 0$ ) is also shown (red online). It accurately describes  $g_0^{zz}(t)$  up to the threshold time. Horizontal line (blue online) marks the long-time average of the autocorrelation function.

take a discrete Fourier transform of the r.h.s. of eq.(11) and use

$$\begin{aligned} \sum_{q \in X_{\text{odd}}} e^{il\varphi(q)} &= \begin{cases} 1 & \text{if } l = jN, j \in \mathbb{Z}, \\ 0 & \text{otherwise,} \end{cases} \\ \sum_{q \in X_{\text{ev}}} e^{il\varphi(q)} &= \begin{cases} (-1)^j & \text{if } l = jN, j \in \mathbb{Z}, \\ 0 & \text{otherwise.} \end{cases} \end{aligned} \quad (14)$$

Formulae (12) have an important advantage compared to formulae (11): infinite sums in (12) may be truncated at some small  $j$  to obtain excellent approximations for times  $t < (j+1)t_{\text{th}}$  with threshold time  $t_{\text{th}} \sim N$ . Thus one may deal with only few terms in eq. (12) in contrast to  $N$  terms in (11). This statement will be proved in full generality in what follows (see Sec. 4 and especially Appendix D.2.2). In two special cases described below one can check it immediately.

### 3.3 Special case: $XX$ chain

When  $\gamma = 0$  functions  $A_j$  and  $B_j$  can be expressed through Bessel functions of the first kind:

$$\begin{aligned} A_j(t) &= (-1)^{Nj/2} \cos(ht) J_{jN}(t), \\ B_j(t) &= (-1)^{Nj/2} \sin(ht) J_{jN}(t). \end{aligned} \quad (15)$$

$J_{jN}(t)$  is negligible for  $t < jN$ , which justifies the truncation of the sums in (12). Threshold time in this case equals  $N$ .

In fact in the case of  $XX$  chain eq. (10) may be further simplified to obtain

$$\begin{aligned} g_n^{zz}(t) &= \frac{1}{2} \left( \left( J_0(t) + 2 \sum_{j=1}^{\infty} J_{jN}(t) \right)^2 + \left( J_0(t) + 2 \sum_{j=1}^{\infty} (-1)^j J_{jN}(t) \right)^2 \right) \\ &= \sum_{j+j'=0 \pmod{2}} J_{jN}(t) J_{j'N}(t). \end{aligned} \quad (16)$$

Note that  $h$  drops out from the final expression. This can be easily seen from the definition (8) of  $g_n^{zz}(t)$  if one recalls that  $\frac{h}{2} \sum_n \sigma_n^z$  commutes with the total Hamiltonian.<sup>1</sup>

Eq. (16) may be used to obtain successive approximations:

$$\begin{array}{c|c}
g_0^{zz}(t) \simeq & \text{for } t \in \\
\hline
J_0^2(t) & [0, N) \\
J_0^2(t) + 4J_N^2(t) & [N, 2N) \\
J_0^2(t) + 4J_N^2(t) + 4J_{2N}^2(t) + 4J_0(t)J_{2N}(t) & [2N, 3N) \\
\vdots & \vdots
\end{array} \tag{17}$$

The first line ( $j = 0$ ) represents a well-known result obtained in thermodynamic ( $N \rightarrow \infty$ ) limit [12]. Approximations in which  $(s+1)$  Bessel functions are kept correspond to  $s$  round trips of a spin wave over the circle. We postpone further discussion of the physical sense of the obtained results to the next section. Exact and approximate expressions for  $g_0^{zz}(t)$  in the  $XX$  chain are plotted at Fig. 2.

Closely related results for the  $XX$  model were obtained in [11]. Namely, they represent one-particle Green function, which is in fact equal to the *zero temperature* correlation function  $g_n^{-+}(t)|_{T=0} \equiv \langle \downarrow \downarrow \dots \downarrow | \sigma_{n+1}^-(t) \sigma_1^+ | \downarrow \downarrow \dots \downarrow \rangle$ , as an infinite sum of Bessel functions.

### 3.4 Special case: Ising chain with $h = 1$

In the case  $h = 1$ ,  $\gamma = 1$  one obtains

$$\begin{aligned}
A_j(t) &= J_{2jN}(2t), \\
B_j(t) &= \frac{1}{2}(J_{2jN+1}(2t) - J_{2jN-1}(2t)) = -J'_{2jN}(2t),
\end{aligned} \tag{18}$$

where prime stands for the derivative. Again  $A_j(t)$  and  $B_j(t)$  are negligible for  $t < jt_{\text{th}}$  with  $t_{\text{th}} = N$ . Successive approximations can be written analogously to the  $XX$  case discussed above.

## 4 Asymptotic approximations

In the present section we derive asymptotic approximations for functions  $A_j, B_j$  which enter eq.(12). As we will see, these approximations physically correspond to taking into account spin waves which wind over the circle  $j$  times. The details of the calculations are presented in Appendix D. Here we outline only major results emphasizing their physical meaning. In the present section we restrict our study to the case  $h \geq 1$ ,  $\gamma \in [0, 1]$ .

### 4.1 Winding of a wave packet over a circle

We approximately calculate  $A_j(t)$  and  $B_j(t)$  using the method of the steepest descent in the plane of complex variable  $\varphi$ . The saddle points for  $A_j$  are obtained from the equation

$$v(\varphi)t - jN = 0, \tag{19}$$

---

<sup>1</sup>As Prof. Perk noted in private communication, another way to explain this fact is to use the transformation into the rotating frame, a procedure familiar in the theory of magnetic resonance.



values of parameters	$\gamma = 0$	$\gamma = 1$		$h = 0$	$h = 1$		$h = 1,$ $\gamma = \sqrt{2 - \sqrt{2}}$
		$h < 1$	$h \geq 1$		$\gamma^2 \in [0, 3/4)$	$\gamma^2 \in [3/4, 1]$	
$\cos \varphi_0$	0	$h$	$1/h$	$-\sqrt{\frac{\gamma}{1+\gamma}}$	$\frac{2\gamma^2+1-\sqrt{4\gamma^2+1}}{2(1-\gamma^2)}$	1	$\sim 0.414$
$V$	1	$h$	1	$1 - \gamma$	$-^*$	$\gamma$	$2(\sqrt{2} - 1)$

\* – bulky (although explicit) expression.

Table 1: Value of maximal group velocity  $V$  in some special cases

where  $v(\varphi) \equiv \partial_\varphi E$  is the group velocity corresponding to momentum  $\varphi$  (the equation corresponding to  $B_j$  is slightly different, see eq.(D-3) in the Appendix D). Note that in general the positions of saddle points depend on time (to be more exact, on the ratio  $t/jN$ ). Two important cases should be distinguished,  $t < jt_{\text{th}}$  and  $t > jt_{\text{th}}$ , where  $t_{\text{th}} \equiv N/V$  and  $V \equiv \sup_\varphi v(\varphi) = v(\varphi_0)$ . In the former case eq.(19) has no real roots and as a consequence  $A_j(t)$  and  $B_j(t)$  are severely suppressed (in accordance with a general result [13]). This explains why one can keep only  $j$  terms in eq.(12) whenever  $t < jt_{\text{th}}$ . If  $h$  is not too close to 1, the suppression law reads

$$A_j(t), B_j(t) \sim \exp[-\text{const} \cdot jN \left( \frac{jt_{\text{th}} - t}{jt_{\text{th}}} \right)^{\frac{3}{2}}], \quad t < jt_{\text{th}}, \quad (20)$$

where the constant is of order of one and depends on  $h$  and  $\gamma$ , see Appendix D.2.2.

In the opposite case  $t > jt_{\text{th}}$  eq.(19) has two real roots and  $A_j(t), B_j(t)$  are not suppressed.

Threshold time  $t_{\text{th}}$  is a time which is necessary for the fastest spin wave to make one round trip over the circle [7]. Thus  $A_j(t)$  and  $B_j(t)$  describe contributions of those parts of the wave packet which have completed exactly  $j$  round trips over the circle. The propagation of the wave packet is visualized in Fig. 3 (see also an analogous figure for the  $XX$  model in [7]). As was shown in [7], initial perturbation localized in the first spin gives rise to two wave packets which travel in opposite directions. Each wave packet is a superposition of all spin waves of corresponding direction. The velocity of the forefronts of these wave packets coincides with the maximal group velocity of the spin waves  $V$ . Therefore as long as  $t < t_{\text{th}} \equiv N/V$ , the wave packets propagate as if the chain were infinite, and the evolution of the first spin is described merely by oscillations in the common tail of the wave packets. This stage of evolution is the only one which may be caught by the  $N \rightarrow \infty$  approximation. Mathematically it is described by keeping only  $j = 0$  terms in eq.(12).

At  $t = t_{\text{th}}$  the forefronts of two wave packets complete the round trip over the circle and meet at the first site. At this moment the regular evolution of the polarization of the first spin is abruptly interrupted by a partial revival. The succeeding evolution between  $t_{\text{th}}$  and  $2t_{\text{th}}$  is determined by the interference between the fastest parts of wave packets which have already made one round trip and the common tail of the wave packets with zero velocity which still stays at the first site. Mathematically this stage is described by keeping  $j = 0, 1$  terms in eq.(12).

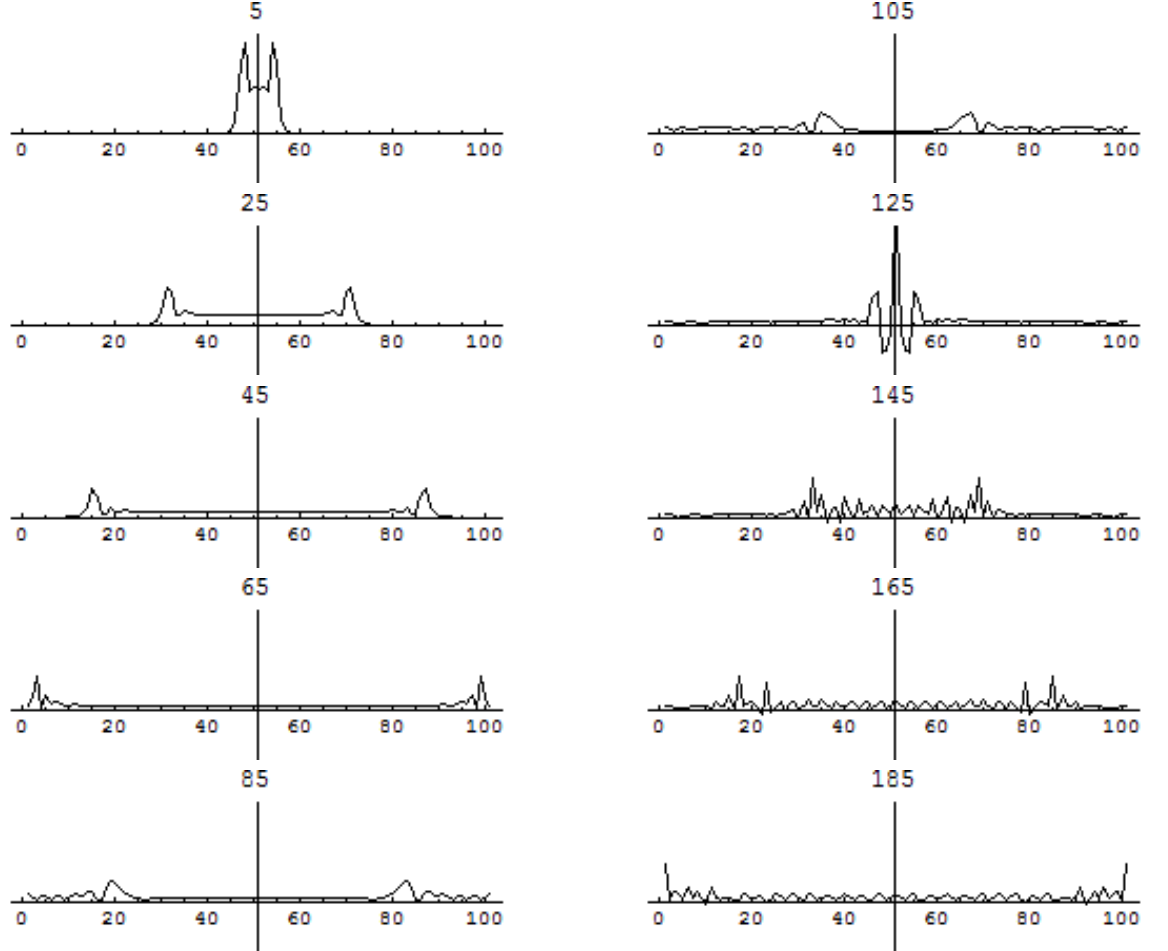


Figure 3: Propagation of two oppositely directed wave packets along the spin chain. Snapshots of polarizations of all spins at times  $t = 5, 25, \dots, 185$  are presented. In this figure the initial perturbation is localized at the 51'st site (in contrast to the rest of the paper), the zeroth site is identified with the hundredth one. The model parameters are  $h = 1$ ,  $\gamma = \sqrt{\sqrt{2} - 1}$ , the threshold time is  $t_{\text{th}} \simeq 117.7$ . Note the emergence of flat polarization plateau which grows up to  $t_{\text{th}}/2$ , then shrinks and completely disappears at threshold time. This feature is specific for the case  $h = 1$ . A three-dimensional plot representing a more generic case (without plateau) of propagation of wave packets along the cyclic  $XX$  chain may be found in [7].

Subsequent stages are described in a similar fashion. The wave packets continue to wind over the circle. At  $st_{\text{th}} < t < (s+1)t_{\text{th}}$  polarization at the first site is a result of interference of waves which completed  $0, 1, \dots, s$  round trips over the circle. This corresponds to keeping  $j = 0, 1, \dots, s$  terms in eq.(12). The revivals at  $t = st_{\text{th}}$  become less pronounced with increasing  $s$  due to the decrease of the maximal amplitude and the smearing of the forefront of the wave packet, see Fig. 3.

Clearly the maximal group velocity  $V$  is an important quantity in the above picture as it determines the threshold time. We show in Appendix C that  $V \in [2(\sqrt{2}-1), 1]$  as long as one restricts himself to the case  $h \geq 1$ . Without this restriction  $V$  is confined to the interval  $[0, 1]$ .  $V = 2(\sqrt{2}-1)$  is achieved at  $h = 1$ ,  $\gamma = \sqrt{\sqrt{2}-1}$  (this case is presented on the upper right plot in Fig. 1). More detailed considerations including several important specific cases may be found in Appendix C.

The above described physical picture of propagation of wave packets and emergence of revivals implies that the forefront of the wave packet is rather sharp. This is indeed true for the following simple reason. As long as  $\varphi_0$  is a point of maximum, a bunch of fermions exists with  $\varphi(q)$  lying in the vicinity of  $\varphi_0$ . The group velocities of these modes are equal to each other and to the maximal velocity  $V$  up to quadratic terms. It is exactly these modes which form the sharp forefront of the wave packet which smears very slowly compared to the rest of the wave packet. Some proposals for high-quality quantum state transfer along spin chains exploit this feature (see e.g. [14]).

## 4.2 Asymptotic approximations for $t < t_{\text{th}}$ .

First we separately consider the case  $t < t_{\text{th}}$  (see Appendix D.1). This case is special because the position of saddle points do not depend on time. Approximations at this time interval coincide with formulas obtained in thermodynamic limit.

Let us introduce a dimensionless parameter  $\epsilon \equiv h - 1$ . Here and in what follows we mainly concentrate on the case where  $h$  is not too close to 1. In this case the method of the steepest descend can be applied straightforwardly, and we obtain an asymptotic approximation for times  $\max\{1, \epsilon^{-1}\} < t < t_{\text{th}}$ :

$$g_0^{zz}(t) \simeq \frac{1}{2\pi t} \cdot ((a_{0+} - a_{0-})^2 + 4a_{0+}a_{0-} \cos^2(t - \frac{\pi}{4})), \quad (21)$$

where

$$a_{0\pm} \equiv \sqrt{\frac{h \pm 1}{h \pm (1 - \gamma^2)}}.$$

Note that  $\epsilon$  should be greater than  $N^{-1}$ , otherwise the time interval at which the approximation is valid vanishes. This restriction is relaxed if  $\gamma \ll \epsilon$ . In the latter case even for  $\epsilon \ll 1$  formula (21) is valid for  $1 \ll t < t_{\text{th}}$ . In fact in this case one may approximate  $g_0^{zz}(t)$  simply by the autocorrelation function for  $\gamma = 0$  which is given by  $J_0^2(t)$  for  $t < t_{\text{th}}$  according to (17).

In the case of small  $\epsilon$  the application of the method of the steepest descend is more sophisticated. The complications are not unexpected because  $h = 1$  is the point of quantum phase transition (QPT) for the XY model. However given certain relations

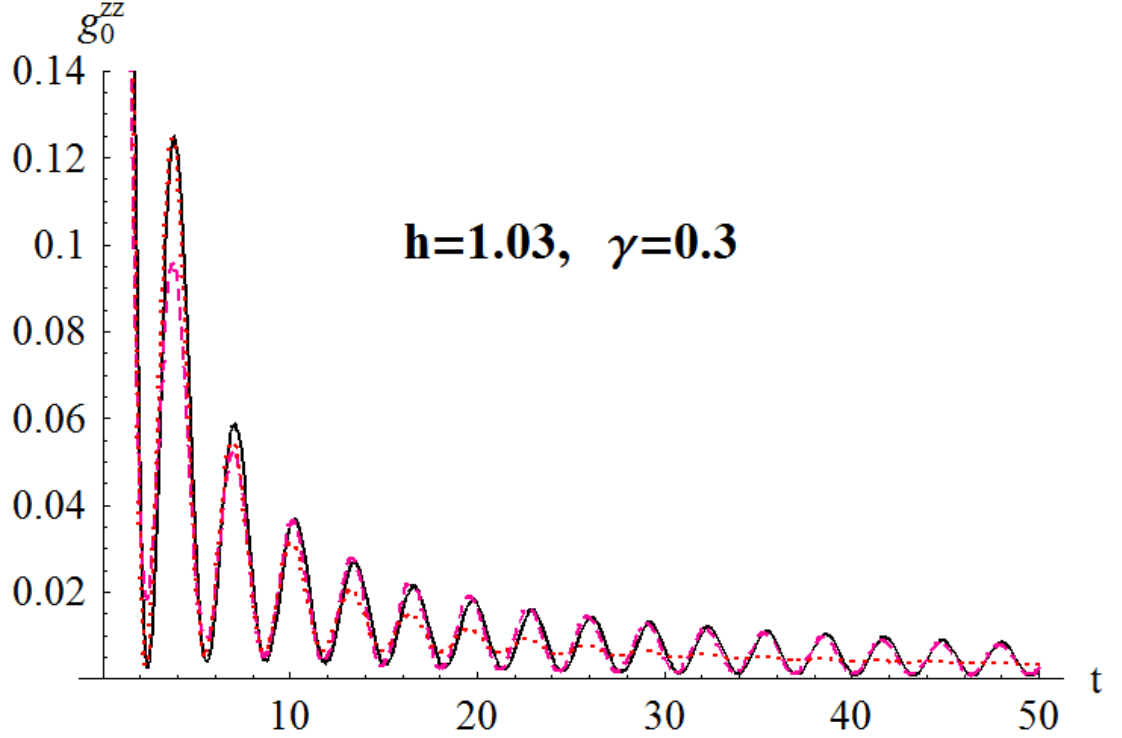


Figure 4: Autocorrelation function  $g_n^{zz}(t)$  at  $t < t_{\text{th}}$  or, equivalently, in thermodynamic limit. Solid line – exact expression, dashed line (magenta online) – asymptotic approximation (21) valid for larger times,  $\epsilon^{-1} < t < t_{\text{th}}$ , dotted line (red online) – asymptotic approximation (22) valid for smaller times,  $1 < t \ll \gamma^2 \epsilon^{-2}$ .

between  $\epsilon$ ,  $\gamma$  and  $N^{-1}$  one may still obtain accurate approximations, see Appendix D.1. For example in the case  $\epsilon^2 \lesssim \gamma^2 \ll 1$  we are able to obtain an asymptotic expression valid for  $1 < t \ll \gamma^2 \epsilon^{-2}$ :

$$g_0^{zz}(t) \simeq \frac{1}{\pi(2 - \gamma^2)t} \left( 1 + \frac{2 - \gamma^2}{2\sqrt{1 - \gamma^2}} \exp\left[-\frac{2\gamma^2}{\sqrt{1 - \gamma^2}}t\right] + 2\sqrt{\frac{2 - \gamma^2}{2\sqrt{(1 - \gamma^2)}}} \exp\left[-\frac{\gamma^2}{\sqrt{1 - \gamma^2}}t\right] \cos\left(2t - \frac{\pi}{4} - \arctan \frac{1}{\sqrt{1 - \gamma^2}}\right) \right) \quad (22)$$

If  $\gamma$  is not too small, the exponents rapidly decrease with time and one is left with non-oscillating decay:

$$g_0^{zz}(t) = \frac{1}{\pi(2 - \gamma^2)t}. \quad (23)$$

For certain values of parameters both asymptotic approximations (21) and (22) may be applicable, but at different time intervals. An example is given in Fig. 4.

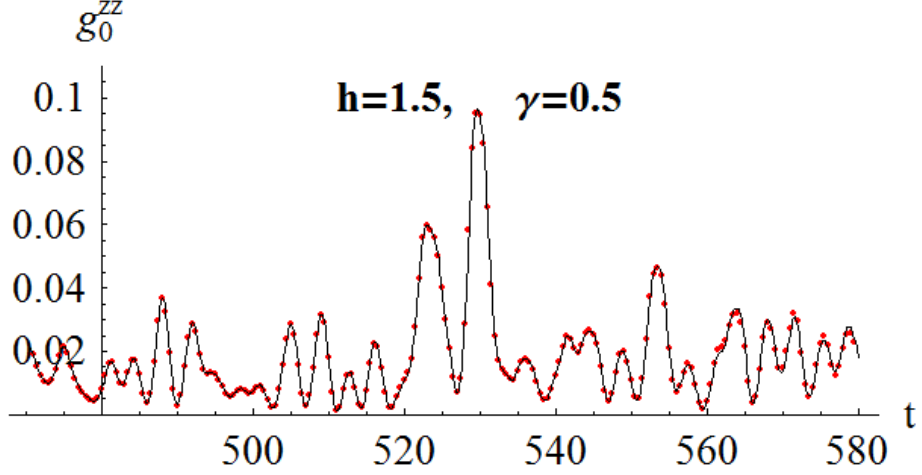


Figure 5: Exact autocorrelation function  $g_0^{zz}(t)$  (solid line) and the approximation corresponding to 5 complete round trips over the circle (points). One can see that the approximation excellently describes both the revival and the apparently chaotic evolution far from the revival.

### 4.3 Asymptotic approximations for $t > jt_{\text{th}}$ .

Now let us turn to asymptotics for functions  $A_j(t)$  and  $B_j(t)$  and corresponding approximations for  $g_0^{zz}(t)$  in case of  $j \geq 1$ . It was already noted that  $A_j(t)$  and  $B_j(t)$  are suppressed for  $t < jt_{\text{th}}$ .

For sufficiently large times and  $h$  not too close to 1 (more explicitly, for  $(t - jt_{\text{th}}) \gg 1$  and  $\epsilon^{-1} \ll jt_{\text{th}}$ ) we obtain (see Appendix D.2.1)

$$A_j(t) \simeq \frac{1}{\sqrt{2\pi t}} \left( \sqrt{\frac{1}{|E''(\varphi_1)|}} \cos(tE(\varphi_1) - jN\varphi_1 + \frac{\pi}{4}) + \sqrt{\frac{1}{|E''(\varphi_2)|}} \cos(tE(\varphi_2) - jN\varphi_2 - \frac{\pi}{4}) + O\left(\frac{1}{t}\right) \right), \quad (24)$$

$$B_j(t) \simeq \frac{1}{\sqrt{2\pi t}} \left( \sqrt{\frac{1}{|E''(\varphi_1)|}} \frac{\varepsilon(\varphi_1)}{E(\varphi_1)} \sin(tE(\varphi_1) - jN\varphi_1 + \frac{\pi}{4}) + \sqrt{\frac{1}{|E''(\varphi_2)|}} \frac{\varepsilon(\varphi_2)}{E(\varphi_2)} \sin(tE(\varphi_2) - jN\varphi_2 - \frac{\pi}{4}) + O\left(\frac{1}{t}\right) \right). \quad (25)$$

Saddle points  $\varphi_{1,2}(t)$  are obtained from Eq. (19). The latter may be reduced to a polynomial equation (D-16) of fourth degree with regard to  $\cos \varphi$ .

These asymptotics being plugged into eq.(12) excellently approximate  $g_0^{zz}(t)$  everywhere but in the vicinity of points  $jt_{\text{th}}$  where revivals occur. In order to describe revival one should use different approximate expressions presented in the next subsection.

The case of small  $\epsilon$  is again more cumbersome. However it can also be treated as is demonstrated in Appendix D.2.1.

#### 4.4 Partial revivals

Above derived approximations based on the method of the steepest descent are not applicable in the vicinity of multiples of  $t_{\text{th}}$  when two saddle points are close to each other and to the point  $\varphi_0$ . However, as long as at  $t = jt_{\text{th}}$  is exactly the time when a partial revival occurs, it is highly desirable to have an approximation which works well for  $t \simeq jt_{\text{th}}$ . We present such an approximation in the Appendix D.2.3. It is based on the fact that in the case under consideration the integrals in the definitions (13) of  $A_j$  and  $B_j$  pick up the major contribution in the vicinity of  $\varphi_0$ . This justifies the expansion of  $E(\varphi)$  in the vicinity of  $\varphi_0$  which leads to the desired approximate expressions. If  $h$  is not too close to 1, namely  $\epsilon \gg \gamma N^{-1}$ , they read

$$\begin{aligned} A_j(t) &\simeq \left( \frac{2}{|E'''(\varphi_0)|t} \right)^{\frac{1}{3}} \cdot \text{Ai} \left[ -N \frac{t-jt_{\text{th}}}{t_{\text{th}}} \left( \frac{2}{|E'''(\varphi_0)|t} \right)^{\frac{1}{3}} \right] \cdot \cos(E(\varphi_0)t - jN\varphi_0) \\ B_j(t) &\simeq \frac{\varepsilon(\varphi_0)}{E(\varphi_0)} \left( \frac{2}{|E'''(\varphi_0)|t} \right)^{\frac{1}{3}} \cdot \text{Ai} \left[ -N \frac{t-jt_{\text{th}}}{t_{\text{th}}} \left( \frac{2}{|E'''(\varphi_0)|t} \right)^{\frac{1}{3}} \right] \cdot \sin(E(\varphi_0)t - jN\varphi_0), \end{aligned} \quad (26)$$

where  $\text{Ai}(x)$  is the Airy function of the first kind and  $\varphi_0$  corresponds to the maximal group velocity. Curiously enough, the above approximation works well even far from  $jt_{\text{th}}$ . Note that as long as  $E'''(\varphi_0)$  does not depend on time in contrast to  $E''(\varphi_{1,2})$ , it is much easier in practice to calculate the r.h.s. of equations (26) than the r.h.s. of eqs. (24), (25). The only disadvantage of the approximation (26) is that we do not analytically control the errors of this approximation; however, numerical calculations show that they are small.

To summarize, in order to approximate the autocorrelation function up to  $(s+1)t_{\text{th}}$ , one should take  $A_0, B_0$  according to eq. (D-7),  $A_j, B_j$  with  $j = 1, 2, \dots, s-1$  according to eqs. (24), (25) and  $A_s, B_s$  according to eq. (26). The resulting expression approximates the autocorrelation function with excellent precision as shown in Fig. 5.

The case when  $h \simeq 1$  is as usual more cumbersome. We do not provide a complete analysis which would be rather bulky, however we derive an approximation for  $h = 1, \gamma^2 \geq 3/4$ , see Appendix D.2.3, eqs. (D-32)–(D-36).

Let us discuss the law which governs the decrease of revival amplitudes. In general the  $s$ 'th partial revival is described by the mutual interference between all  $A_j(t)$  with  $j = 0, 1, \dots, s$  and mutual interference between all  $B_j(t)$  with  $j = 0, 1, \dots, s$ . However as a first approximation one may consider only  $A_s(t)$  and  $B_s(t)$  which give the leading contribution.  $A_j(t)$  in eq.(26) decreases as  $t^{-1/3}$ , while in eq. (24) – as  $t^{-1/2}$ . This means that the amplitude of revivals decreases more slowly than the averaged value of  $g_0^{zz}(t)$  between revivals. In fact this makes the revivals so visible against the background. As a result for  $h - 1 > \gamma/N$  one gets from eq.(26) the following law:

$$g_0^{zz}|_{s'\text{th revival}} \sim (sN)^{-2/3} \quad (27)$$

This law work satisfactory for sufficiently large number of spins and for moderate  $s$ . In particular, as long as the long-time average of  $g_0^{zz}$  is of order of  $N^{-1}$ , this law can not be valid for  $s \gtrsim \sqrt{N}$ . In fact it breaks down somewhat earlier because at large  $s$  contributions from  $A_j, B_j$  with  $j < s$  start to contribute significantly. Our numerical calculation show that for 10000 spins the above law is reliable for a few dozens of revivals.

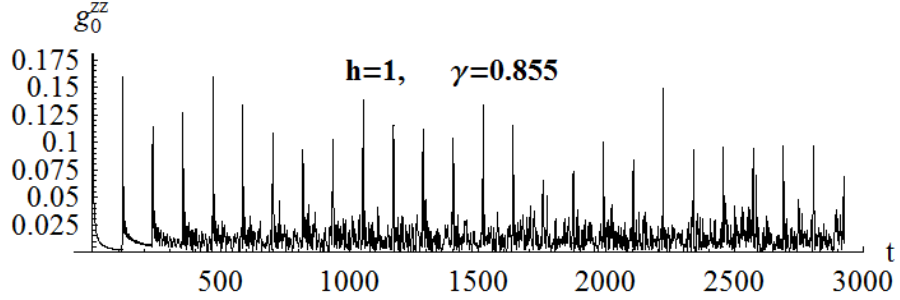


Figure 6: Extremely pronounced revivals occur in otherwise apparently chaotic regime in the small region of the parameter space in the vicinity of the point  $h = 1, \gamma^2 = 3/4$ . Threshold time here is  $t_{\text{th}} \simeq 117$ .

For more moderate number of spins,  $N \sim 100$ , the law is quickly distorted due to the above mentioned contribution from  $A_j(t)$  and  $B_j(t)$  with  $j < s$ . In particular, maxima of revivals do not decrease monotonically in this case, see Fig. 6.

Noteworthy, when  $h = 1$  and  $\gamma^2 = 3/4$  the amplitudes of the revivals decrease even more slowly than implied by eq. (27), namely

$$g_0^{zz}|_{s' \text{th revival}} \sim (sN)^{-2/5}, h = 1, \gamma^2 = 3/4, \quad (28)$$

see Appendix D.2.3 and especially eq. (D-36) for the details. Again this law works for sufficiently large number of spins. However the fact that the  $h = 1, \gamma^2 = 3/4$  point of a parameter space is a special one reveals itself already for modest  $N \sim 100$ : the revivals appear to be especially pronounced in the vicinity of this point (see fig. 6), although they do not decrease monotonically due to the above discussed interference of  $A_j, B_j$  with different  $j$ . A very similar effect was observed previously in [15]. Namely, it was numerically discovered that when a perturbation propagates from one end of an open-ended  $XY$  chain to another, the attenuation of the amplitude of a wave packet is minimal for  $h = 1, \gamma \simeq 0.7$ .

## 5 Transition from regular to chaotic evolution

Plots of  $g_n^{zz}(t)$  presented in the present paper clearly demonstrate that transition from regular to chaotic evolution is a general feature of spin dynamics. In the present section we provide a discussion of this fact on a qualitative level. More thorough study including quantitative considerations will be presented elsewhere.

From Fig. 2 it is evident that the spin evolution is apparently regular at small times but apparently chaotic at large times, threshold time  $t_{\text{th}}$  determining the relevant timescale. However it is not so easy to define the terms "regular" and "chaotic" rigorously in the present context. One should especially be cautious when using the term "chaos" here. It is well known that the notion of chaos in quantum systems is not uniquely defined (see e.g. [16]). One widely used definition of quantum chaos is based on energy level repulsion. According to this particular definition  $XY$  model is certainly *not* chaotic because it is

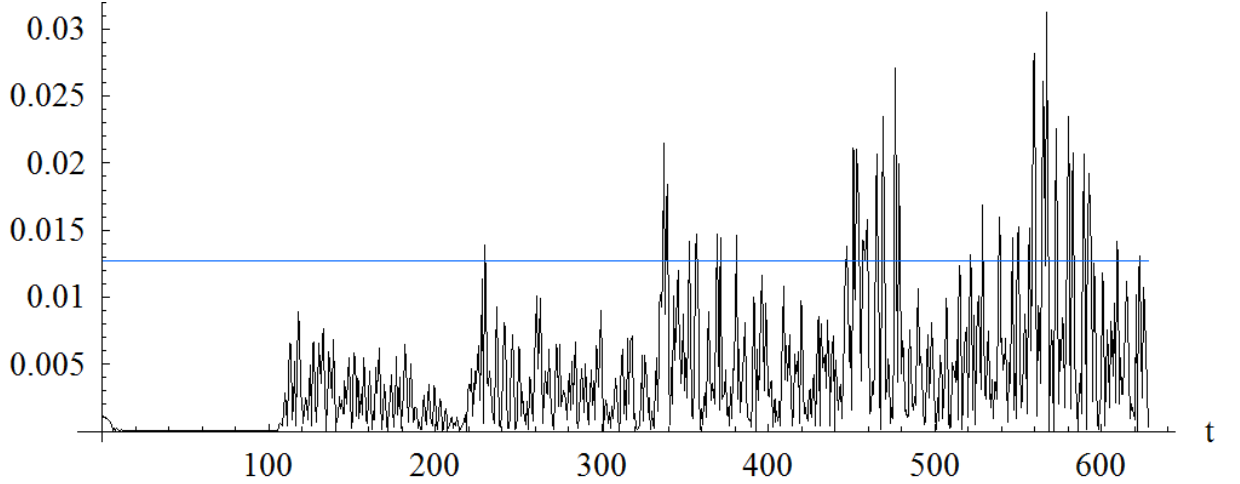


Figure 7: Sensitivity of the correlation function to the small variation of  $\gamma$ . Function plotted is the absolute value of difference of two correlation functions  $g_0^{zz}(t)$  corresponding to two slightly different values of anisotropy parameter:  $|g_0^{zz}(t)_{\gamma=0.5} - g_0^{zz}(t)_{\gamma=0.505}|$ . Magnetic field in both cases is  $h = 1$ , number of spins  $N = 100$ . Threshold time is approximately 112. The horizontal line (blue online) shows the value which the above difference would admit if the two functions were absolutely uncorrelated.

integrable and thus its level statistics is Poissonian (i.e. non-repulsive). In what follows we briefly discuss two distinct approaches which may be used to describe the level of irregularity of  $g_n^{zz}(t)$ .

The first approach is based on the physical picture of winding of the wave packet over the circle and exploits asymptotic approximations derived above. In this approach we pragmatically consider the evolution to be regular at some interval of time if the correlation function may be well approximated by a linear combination of *few* ( $\ll N$ ) oscillating functions with different frequencies (probably multiplied by a power-law prefactor) at this interval. Conversely, the evolution is considered to be chaotic when the approximation involves many ( $\sim N$ ) harmonics. The first stage of evolution ( $t < t_{\text{th}}$ ) is the most regular one: according to eqs. (21),(22) it is described by a single cosine. At times  $t_{\text{th}}, 2t_{\text{th}}, 3t_{\text{th}}$  new functions  $A_j, B_j$  come into play in eq.(12) and the number of harmonics increases stepwise. Thus the level of irregularity also increases. This does not last forever: according to eq.(10)  $N$  harmonics is enough to describe  $g_0^{zz}(t)$  *exactly*. Evidently the largest possible level of irregularity is achieved not later than at  $t = Nt_{\text{th}}$ . Note that here we use the term "harmonics" in a slightly non-standard way: we do not demand that the corresponding frequencies should be multiples of a single, minimal frequency. The described approach resembles the Feigenbaum rout to chaos through period doubling (see e.g. [17]). However in the case under consideration there is no *doubling* – the relation between frequencies of new harmonics switching on at certain times is not so evident. Moreover, these frequencies may even be slowly varying in time. The Fourier analysis of the correlation function at different time intervals is necessary to obtain more quantitative picture. This will be done elsewhere.



In the second approach one examines the level of sensitivity of  $g_n^{zz}(t)$  to small variations of Hamiltonian parameters  $h$  and  $\gamma$ . This approach introduced in [18] resembles the definition of classical chaos through the extreme sensitivity to initial conditions. We visualize the sensitivity of  $g_n^{zz}(t)$  to small variations of  $\gamma$  in Fig. 7. One can see that during the regular stage of evolution ( $t < t_{\text{th}}$ ) such sensitivity is small, while at large times ( $t > \text{few} \cdot t_{\text{th}}$ ) it is comparable to what one could expect if two correlation functions with slightly different parameters were absolutely mutually uncorrelated. As in the previous approach, the rate of thus defined chaoticity increases stepwise at times which are multiples of  $t_{\text{th}}$ , the first step occurring at  $t = t_{\text{th}}$  being especially pronounced, see Fig. 7. Curiously, our numerical experiments indicate that the sensitivity of  $g_n^{zz}(t)$  to variations of  $h$  and  $\gamma$  generically tends to be larger in the vicinity of quantum phase transition line  $h = 1$ . It would be quite surprising if this relation between QPT and chaoticity of the correlation function is confirmed, since the correlation function is calculated at infinite temperature while QPT occurs at zero temperature.

## 6 Discussion and conclusions

If one merely plots the evolution of spin polarization in the finite cyclic  $XY$  chain for various values of Hamiltonian parameters, one immediately discovers that the spin dynamics exhibits a variety of peculiar features. Previous studies [6, 7] and the present study reveal the following physical picture.

- A threshold time exists up to which the polarization of a given spin evolves as if the chain were infinite. This is the time necessary for the fastest spin wave to make a round trip over the cyclic chain. Up to the threshold time the evolution is regular (for  $h \geq 1$ ).
- At the threshold time the regular evolution is interrupted by a partial revival. Subsequent partial revivals occur at  $2t_{\text{th}}, 3t_{\text{th}}, \dots$ . Generically the evolution becomes more and more irregular (chaotic) after each partial revival. This picture may be explained on the basis of eqs.(12) in which terms  $A_j(t), B_j(t)$  start contributing to the sums at  $t = jt_{\text{th}}$ . Physically this picture may be understood as the interference between the forefront of the wave packet which have made  $j$  round trips over the chain and its lagging tail.

Our main result is as follows. We have expressed the autocorrelation function  $g_0^{zz}(t)$  through infinite sums of functions  $A_j(t), B_j(t)$  over the winding number  $j$ . This expression allows to write down successive approximations for  $g_0^{zz}(t)$ . For any given  $j$  the  $j$ th approximation takes into account  $j$  complete round trips of the wave packet and consequently may be applied up to  $t = (j + 1)t_{\text{th}}$ . Functions  $A_j(t)$  and  $B_j(t)$  are defined in integral form. In two special cases ( $\gamma = 0$  and  $\gamma = 1, h = 1$ ) they can be expressed through Bessel functions. In a general case we are able to provide very accurate approximations to these functions valid at various times and in various regions of parameter space. These approximation are obtained using methods of complex analysis, in particular, the method of the steepest descent.

We have shown that the amplitude of the revivals decreases slower than the average amplitude of the correlation function between two revivals. This fact makes the revivals clearly visible against the background. We have analytically shown that the most pronounced revivals are observed in a vicinity of a special point of the parameter space ( $h = 1$ ,  $\gamma^2 = 3/4$ ). Previously this was observed numerically in an open-ended chain [15].

A striking feature of the dynamics in the finite spin chain is the transition from regular to chaotic evolution. In the present paper we have restricted ourselves by brief and qualitative discussion of the nature and origin of this transition. Further work is necessary to give a more exhaustive and quantitative analysis.

We also have observed a feature concerning long-time properties of evolution. It was shown in [7] that in the  $XX$  model the polarization of any spin never changes its sign provided the initial conditions are specified by eq. (7). We point out that in the  $XY$  model this property still holds for the *first* spin (distinguished by the initial conditions) but does not hold for any other spin. Thus the first spin retains the memory of the fact that it was distinguished by the initial conditions forever. Moreover, its time-averaged polarization differs from the time-averaged polarization of any other spin which was already noted in the context of the  $XX$  model [7]. Thus we encounter the absence of the complete thermalization which is, however, only a finite-size effect (scaling as  $1/N$ ).

## Acknowledgements

The authors acknowledge the enlightening comments by J.H.H. Perk and L. Banchi and the fruitful discussion at the Condensed Matter Theory seminar at ITAE RAS, especially valuable remarks made by A.L. Rakhmanov concerning signatures of chaos in the  $XY$  model. O.L. also thanks E. Bogomolny and O. Giraud for useful discussions. O.L. is grateful to ERC (grant no. 279738 NEDFOQ) for financial support. The partial support from grants NSh-4172.2010.2, RFBR-11-02-00778, RFBR-10-02-01398 and from the Ministry of Education and Science of the Russian Federation under contracts N<sup>o</sup>N<sup>o</sup> 02.740.11.5158, 02.740.11.0239 is also acknowledged.

## A Diagonalization of finite cyclic $XY$ spin chain

### A.1 Ranges of parameters

Let us rewrite the Hamiltonian we are going to diagonalize:

$$H(h, \gamma, \kappa) = \frac{\kappa}{4} \sum_{n=1}^N ((1 + \gamma)\sigma_n^x \sigma_{n+1}^x + (1 - \gamma)\sigma_n^y \sigma_{n+1}^y) + \frac{h}{2} \sum_{n=1}^N \sigma_n^z, \quad (\text{A-1})$$

where indices 1 and  $N + 1$  are identified, and  $N$  is even. Here we have introduced coupling constant  $\kappa$ , which is taken to be 1 everywhere in the article but this subsection. Let us show that one may consider  $h, \gamma, \kappa \geq 0$  without loss of generality. This means that one can change the sign of each constant by means of local unitary transformation  $U$ . These transformations correspond merely to rotations of the coordinate systems at each spin site.

To change sign of  $h$  one can transform  $\sigma_n^y \rightarrow -\sigma_n^y$ ,  $\sigma_n^z \rightarrow -\sigma_n^z$  at each spin site  $n$ :

$$U = \prod_{n=1}^N e^{i\sigma_n^x \pi/2} = \prod_{n=1}^N i\sigma_n^x,$$

$$U^\dagger \sigma_n^x U = \sigma_n^x, \quad U^\dagger \sigma_n^y U = -\sigma_n^y, \quad U^\dagger \sigma_n^z U = -\sigma_n^z, \quad U^\dagger H(h, \gamma, \kappa) U = H(-h, \gamma, \kappa). \quad (\text{A-2})$$

Analogously, to change sign of  $\gamma$  one transforms  $\sigma_n^x \rightarrow \sigma_n^x$ ,  $\sigma_n^y \rightarrow -\sigma_n^y$  at each site  $n$  by means of  $U = \prod_{n=1}^N e^{i\sigma_n^z \pi/4}$ .

To change sign of  $\kappa$  one transforms  $\sigma_{2m}^x \rightarrow -\sigma_{2m}^x$ ,  $\sigma_{2m}^y \rightarrow -\sigma_{2m}^y$  at each *even* site  $2m$  by means of  $U = \prod_{m=1}^{N/2} e^{i\sigma_{2m}^z \pi/2}$ .

As soon as sign of  $\kappa$  is unimportant, one may put  $\kappa = 1$ .

## A.2 $H$ in terms of $\sigma_n^\pm$

We define the operators  $\sigma_n^\pm$  in a usual way,

$$\sigma_n^+ = \frac{1}{2}(\sigma_n^x + i\sigma_n^y), \quad \sigma_n^- = \frac{1}{2}(\sigma_n^x - i\sigma_n^y). \quad (\text{A-3})$$

These operators are neither Bose nor Fermi operators:

$$\sigma_n^+ \sigma_n^- + \sigma_n^- \sigma_n^+ = 1, \quad (\text{A-4})$$

$$\sigma_m^+ \sigma_n^- = \sigma_n^- \sigma_m^+ \quad \text{for } m \neq n. \quad (\text{A-5})$$

The following simple equalities prove to be useful:

$$\sigma^z = 2\sigma^+ \sigma^- - 1 = -2\sigma^- \sigma^+ + 1 \quad (\text{A-6})$$

$$\sigma^z \sigma^+ = -\sigma^+ \sigma^z = \sigma^+, \quad \sigma^z \sigma^- = -\sigma^- \sigma^z = -\sigma^- \quad (\text{A-7})$$

The Hamiltonian may be rewritten in terms of  $\sigma_n^\pm$  as follows:

$$H = H_0 + H_\gamma + H_h \quad (\text{A-8})$$

with

$$H_0 = \frac{1}{2} \sum_{n=1}^N (\sigma_n^+ \sigma_{n+1}^- + \sigma_n^- \sigma_{n+1}^+), \quad (\text{A-9})$$

$$H_\gamma = \frac{\gamma}{2} \sum_{n=1}^N (\sigma_n^+ \sigma_{n+1}^+ + \sigma_n^- \sigma_{n+1}^-), \quad (\text{A-10})$$

$$H_h = h \sum_{n=1}^N \sigma_n^+ \sigma_n^- - Nh/2. \quad (\text{A-11})$$

### A.3 Jordan-Wigner transformation

Define the operators

$$\Pi_n \equiv \prod_{n=1}^n \sigma_n^z. \quad (\text{A-12})$$

Evidently,  $\Pi_N$  coincides with the parity operator  $\Pi$  defined in Sec. 2.

Define Fermi operators  $a_n^-$ ,  $a_n^+$  as follows

$$a_n^- \equiv \sigma_n^- \Pi_{n-1} = \Pi_{n-1} \sigma_n^-, \quad a_n^+ \equiv \sigma_n^+ \Pi_{n-1} = \Pi_{n-1} \sigma_n^+ \quad (\text{A-13})$$

This implies

$$\sigma_n^- = a_n^- \Pi_{n-1} = \Pi_{n-1} a_n^-, \quad \sigma_n^+ = a_n^+ \Pi_{n-1} = \Pi_{n-1} a_n^+, \quad (\text{A-14})$$

$$\{a_m^+, a_n^-\} = \delta_{mn}, \quad \{a_m^+, a_n^+\} = \{a_m^-, a_n^-\} = 0, \quad (\text{A-15})$$

$$\sigma_n^z = 2a_n^+ a_n^- - 1 = -2a_n^- a_n^+ + 1. \quad (\text{A-16})$$

The Hamiltonian takes the form (note that now the ordering of  $a_n^\pm$ ,  $a_{n+1}^\pm$  is important; also note the change of the total sign):

$$H_0 = -\frac{1}{2} \left[ \sum_{n=1}^N (a_n^+ a_{n+1}^- + a_{n+1}^+ a_n^-) - (1 + \Pi)(a_N^+ a_1^- + a_1^+ a_N^-) \right]. \quad (\text{A-17})$$

$$H_\gamma = -\frac{\gamma}{2} \left[ \sum_{n=1}^N (a_n^+ a_{n+1}^+ + a_{n+1}^- a_n^-) - (1 + \Pi)(a_N^+ a_1^+ + a_1^- a_N^-) \right]. \quad (\text{A-18})$$

$$H_h = h \sum_{n=1}^N a_n^+ a_n^- - Nh/2. \quad (\text{A-19})$$

### A.4 Fourier transformation

Define for arbitrary real  $q$

$$b_q^- \equiv \frac{e^{i\pi/4}}{\sqrt{N}} \sum_{n=1}^N e^{-2\pi i q(n-1)/N} a_n^-, \quad b_q^+ \equiv \frac{e^{-i\pi/4}}{\sqrt{N}} \sum_{n=1}^N e^{2\pi i q(n-1)/N} a_n^+, \quad (\text{A-20})$$

Then

$$\{b_k^+, b_q^+\} = \{b_k^-, b_q^-\} = 0, \quad \{b_k^+, b_q^-\} = \frac{1}{N} \frac{1 - e^{2\pi i(k-q)}}{1 - e^{2\pi i(k-q)/N}}. \quad (\text{A-21})$$

In particular, if one takes

$$q = -\frac{N}{2} + 1, \quad -\frac{N}{2} + 2, \dots, \frac{N}{2} \quad (X_{\text{odd}}) \quad (\text{A-22})$$

or

$$q = -\frac{N}{2} + \frac{1}{2}, \quad -\frac{N}{2} + \frac{3}{2}, \dots, \frac{N}{2} - \frac{1}{2} \quad (X_{\text{ev}}) \quad (\text{A-23})$$

then the set of  $b_q^-$  is the set of Fermi annihilation operators.

The Hamiltonian may be written in terms of  $b_q^\pm$  as follows:

$$H = H^{\text{odd}} P^{\text{odd}} + H^{\text{ev}} P^{\text{ev}} \quad (\text{A-24})$$

with

$$P^{\text{odd}} \equiv (1 - \Pi)/2, \quad P^{\text{ev}} \equiv (1 + \Pi)/2, \quad (\text{A-25})$$

$$H^{\text{ev}} = \sum_{q=1/2}^{N/2-1/2} H_q, \quad H^{\text{odd}} = \sum_{q=1}^{N/2-1} H_q + H_{0,N/2}, \quad (\text{A-26})$$

$$H_q = (h - \cos \varphi(q)) (b_q^+ b_q^- + b_{-q}^+ b_{-q}^-) + \gamma \sin \varphi(q) (b_q^+ b_{-q}^+ + b_{-q}^- b_q^-) - h, \quad \varphi(q) \equiv 2\pi q/N \quad (\text{A-27})$$

and

$$H_{0,N/2} = (h - 1)b_0^+ b_0^- + (h + 1)b_{N/2}^+ b_{N/2}^- - h. \quad (\text{A-28})$$

## A.5 Bogolyubov transformation

Define the following quantities

$$\Gamma_q \equiv \gamma \sin \varphi(q), \quad \varepsilon_q \equiv h - \cos \varphi(q), \quad E_q \equiv \sqrt{\varepsilon_q^2 + \Gamma_q^2}, \quad (\text{A-29})$$

Each  $H_q$  may be written as follows:

$$H_q = \begin{pmatrix} b_q^+ & b_{-q}^- \end{pmatrix} \begin{pmatrix} \varepsilon_q & \Gamma_q \\ \Gamma_q & -\varepsilon_q \end{pmatrix} \begin{pmatrix} b_q^- \\ b_{-q}^+ \end{pmatrix}. \quad (\text{A-30})$$

It is possible to diagonalize this matrix through Bogolyubov transformation

$$c_q^- = \cos \frac{\theta_q}{2} b_q^- + \sin \frac{\theta_q}{2} b_{-q}^+. \quad (\text{A-31})$$

The diagonalization condition reads  $\tan \theta_q = \Gamma_q / \varepsilon_q$ , and we choose

$$\theta_q \equiv \arctan \frac{\Gamma_q}{\varepsilon_q} \quad \text{for all } q \neq 0. \quad (\text{A-32})$$

This transformation preserves the anticommutation relations.  $H_{0,N/2}$  requires special treatment, which leads to  $\theta_{N/2} = 0$ ,

$$\theta_0 = \begin{cases} 0, & h \geq 1, \\ \pi, & 0 \leq h < 1. \end{cases} \quad (\text{A-33})$$

The inverse transformation reads

$$b_q^- = \cos \frac{\theta_q}{2} c_q^- - \sin \frac{\theta_q}{2} c_{-q}^+ \quad (\text{A-34})$$

The odd and even parts of the Hamiltonian take the form

$$H^{\text{odd (ev)}} = \sum_{q \in X_{\text{odd (ev)}}} E_q (c_q^+ c_q^- - \frac{1}{2}). \quad (\text{A-35})$$

This completes the diagonalization.

## A.6 Eigenstates

Let us first prove the existence of the Fock vacuum states with respect to the annihilation operators  $c_q^-$ , i.e. the states  $|\text{vac}\rangle_{\text{odd}}$ ,  $|\text{vac}\rangle_{\text{ev}}$  which satisfy

$$c_q^- |\text{vac}\rangle_{\text{odd (ev)}} = 0 \quad \forall q \in X_{\text{odd (ev)}}. \quad (\text{A-36})$$

Evidently it is sufficient to prove that

$$\prod_{q \in X_{\text{odd (ev)}}} c_q^- \neq 0. \quad (\text{A-37})$$

If this condition is fulfilled, one can always choose some states  $|\Psi_{\text{odd(ev)}}\rangle$  and normalization constants  $\aleph_{\text{ev}}$  such that

$$|\text{vac}\rangle_{\text{odd}} = \aleph_{\text{odd}} c_{-N/2+1}^- c_{-N/2+2}^- \dots c_{N/2}^- |\Psi_{\text{odd}}\rangle, \quad (\text{A-38})$$

$$|\text{vac}\rangle_{\text{ev}} = \aleph_{\text{ev}} c_{-N/2+1/2}^- c_{-N/2+3/2}^- \dots c_{N/2-1/2}^- |\Psi_{\text{ev}}\rangle. \quad (\text{A-39})$$

The equality

$$\{c_{-N/2+1}^+, [c_{-N/2+2}^+, \{\dots, \{c_{N/2-1}^+, [c_{N/2}^+ \prod_{q \in X_{\text{odd}}} c_q^-] \dots\}] \dots\} = 1 \quad (\text{A-40})$$

and the analogous equality for  $q \in X_{\text{odd (ev)}}$  prove eq.(A-37). Note that  $|\text{vac}\rangle_{\text{ev}}$  is indeed an eigenstate of the Hamiltonian, while  $|\text{vac}\rangle_{\text{odd}}$  is not.

All the eigenstates of the Hamiltonian are obtained from the vacuum states by applying the creation operators  $c_q^+$ . To create the odd number of fermions one should use  $q \in X_{\text{odd}}$  and  $|\text{vac}\rangle_{\text{odd}}$ , while to create the even number of fermions one should use  $q \in X_{\text{ev}}$  and  $|\text{vac}\rangle_{\text{ev}}$ .

Evidently one can enumerate all the eigenstates of the Hamiltonian by the multiindexes

$$Q_M \equiv \{q_1, q_2, \dots, q_M\}, \quad 0 \leq M \leq N, \quad (\text{A-41})$$

with the ordering  $q_1 < q_2 < \dots < q_M$ . Then an eigenstate with  $M$  fermions reads

$$|Q_M\rangle \equiv c_{q_M}^+ \dots c_{q_2}^+ c_{q_1}^+ |\text{vac}\rangle_{\text{odd(ev)}} \quad (\text{A-42})$$

with  $q_1, q_2, \dots, q_M \in X_{\text{odd (ev)}}$  when  $M$  is odd (even). The corresponding eigenenergy reads

$$E_{Q_M} \equiv \sum_{q \in Q_M} E_q - \frac{1}{2} \sum_{q \in X_{\text{odd (ev)}}} E_q. \quad (\text{A-43})$$

For our purposes we need only the matrix elements between the states with the same parity, therefore we use the notation  $|\text{vac}\rangle$  without subscripts in what follows.

## B Calculation of $g_n^{zz}(t)$

To calculate the correlation function at infinite temperature,

$$g_n^{zz}(t) = 2^{-N} \sum_{Q, \tilde{Q}} \langle Q | \sigma_1^z | \tilde{Q} \rangle \langle \tilde{Q} | \sigma_{n+1}^z | Q \rangle e^{-i(E_Q - E_{\tilde{Q}})t}, \quad (\text{B-1})$$

one needs to calculate the corresponding matrix elements. To do this one uses

$$a_{n+1}^+ a_{n+1}^- = \frac{1}{N} \sum_{p, \tilde{p}} \cos \frac{\theta_{\tilde{p}}}{2} \sin \frac{\theta_p}{2} c_{\tilde{p}}^+ c_p^+ e^{-2\pi i(p+\tilde{p})n/N} + \sin \frac{\theta_{\tilde{p}}}{2} \cos \frac{\theta_p}{2} c_{\tilde{p}}^- c_p^- e^{2\pi i(p+\tilde{p})n/N} + \cos \frac{\theta_{\tilde{p}}}{2} \cos \frac{\theta_p}{2} c_{\tilde{p}}^+ c_p^- e^{2\pi i(p-\tilde{p})n/N} + \sin \frac{\theta_{\tilde{p}}}{2} \sin \frac{\theta_p}{2} c_{\tilde{p}}^- c_p^+ e^{-2\pi i(p-\tilde{p})n/N}. \quad (\text{B-2})$$

Here  $p, \tilde{p}$  can run *either* through  $X_{\text{odd}}$  *or* through  $X_{\text{ev}}$  – the expression is valid in both cases. Now it can be easily seen that only three types of matrix elements do not vanish:

1. Diagonal matrix elements.

$$\langle Q | \sigma_{n+1}^z | Q \rangle = \frac{1}{N} \sum_{p \in X_M} \eta(Q_M, p) \cos \theta_p. \quad (\text{B-3})$$

Here  $\eta(Q_M, p) = 1$  if  $p \in Q_M$  and  $-1$  otherwise;  $X_M = X_{\text{odd}}$  (ev) if  $M$  is odd (even).

2. Matrix elements between two states with equal number of fermions, differing by one fermion momentum.

$$Q_M = K_{M-1} \cup \{p\}, \quad \tilde{Q}_M = K_{M-1} \cup \{\tilde{p}\}, \quad p, \tilde{p} \notin K_{M-1}, \quad p \neq \tilde{p} : \\ \langle \tilde{Q} | \sigma_{n+1}^z | Q \rangle = e^{2\pi i(p-\tilde{p})n/N} \frac{2}{N} \cos \frac{\theta_p + \theta_{\tilde{p}}}{2} \langle \tilde{Q} | c_{\tilde{p}}^+ c_p^- | Q \rangle, \quad (\text{B-4})$$

where  $\langle \tilde{Q} | c_{\tilde{p}}^+ c_p^- | Q \rangle = \pm 1$ , depending on the signature of the corresponding permutation. Note that this sign is not important for calculation of  $g_n^{zz}(t)$ .

3. Matrix elements between two states one of which can be obtained from another by addition of two fermions.

$$Q_M = \tilde{Q}_{M-2} \cup \{p\} \cup \{\tilde{p}\}, \quad p, \tilde{p} \notin \tilde{Q}_{M-2}, \quad p \neq \tilde{p} : \\ \langle \tilde{Q} | \sigma_{n+1}^z | Q \rangle = \langle Q | \sigma_{n+1}^z | \tilde{Q} \rangle^* = -\frac{2}{N} e^{2\pi i(p+\tilde{p})n/N} \sin \frac{\theta_p - \theta_{\tilde{p}}}{2} \langle \tilde{Q} | c_{\tilde{p}}^- c_p^- | Q \rangle. \quad (\text{B-5})$$

Now let us sum in eq. (B-1) separately over each type of matrix element:

1. Sum over  $Q = \tilde{Q}$  gives

$$2^{-N} \left( \frac{1}{N^2} \sum_{p, \tilde{p} \in X_{\text{odd}}} \cos \theta_p \cos \theta_{\tilde{p}} \sum_{\text{odd } M} \sum_{Q_M} \eta(Q_M, p) \eta(Q_M, \tilde{p}) + \{\text{odd} \rightarrow \text{even}\} \right) \\ = \frac{1}{2N^2} \left( \sum_{p \in X_{\text{odd}}} + \sum_{p \in X_{\text{ev}}} \right) \cos^2 \theta_p. \quad (\text{B-6})$$

2. Sum over pairs  $(Q, \tilde{Q})$  of the form  $Q = K \cup \{p\}$ ,  $\tilde{Q} = K \cup \{\tilde{p}\}$  gives

$$\frac{1}{2N^2} \left( \sum_{\substack{p, q \in X_{\text{odd}} \\ p \neq \tilde{p}}} + \sum_{\substack{p, q \in X_{\text{ev}} \\ p \neq \tilde{p}}} \right) e^{2\pi i(p-\tilde{p})n/N - i(E_p - E_{\tilde{p}})t} \cos^2 \frac{\theta_p + \theta_{\tilde{p}}}{2}. \quad (\text{B-7})$$

3. Sum over pairs  $(Q, \tilde{Q})$  of the form  $Q = K \cup \{p\} \cup \{\tilde{p}\}$ ,  $\tilde{Q} = K$  gives

$$\frac{1}{4N^2} \left( \sum_{p, q \in X_{\text{odd}}} + \sum_{p, q \in X_{\text{ev}}} \right) e^{2\pi i(p+\tilde{p})n/N - i(E_p + E_{\tilde{p}})t} \sin^2 \frac{\theta_p - \theta_{\tilde{p}}}{2}, \quad (\text{B-8})$$

while summation over  $Q = K$ ,  $\tilde{Q} = K \cup \{p\} \cup \{\tilde{p}\}$  gives a complex conjugated contribution.

If one takes  $p = q$  in expression (B-7), it becomes equal to the (B-6) contribution. Exploiting this one readily obtains

$$g_n^{zz}(t) = \frac{1}{2N^2} \left( \sum_{p, q \in X_{\text{odd}}} + \sum_{p, q \in X_{\text{ev}}} \right) \left( \cos \left( \frac{2\pi(p-\tilde{p})n}{N} - (E_p - E_{\tilde{p}})t \right) \cos^2 \frac{\theta_p + \theta_{\tilde{p}}}{2} + \cos \left( \frac{2\pi(p+\tilde{p})n}{N} - (E_p + E_{\tilde{p}})t \right) \sin^2 \frac{\theta_p - \theta_{\tilde{p}}}{2} \right) \quad (\text{B-9})$$

It can be straightforwardly verified that this expression leads to eqs. (10),(11).

Eq. (B-9) can be used to find a long-time average of the autocorrelation function  $\overline{g_0^{zz}} \equiv \lim_{T \rightarrow \infty} T^{-1} \int_0^T g_0^{zz}(t) dt$ . Let us assume that there are no degeneracies in  $E_q$  other than the mirror degeneracy  $E_q = E_{-q}$  (in other words, that  $E_q = E_p$  implies  $|q| = |p|$ ). This is a generic case. Then

$$\overline{g_0^{zz}} = \frac{1}{N} \left( 1 - \frac{1}{N} + \frac{1}{2N} \left( \sum_{p \in X_{\text{odd}}} + \sum_{p \in X_{\text{ev}}} \right) \cos^2 \theta_p \right). \quad (\text{B-10})$$

Term  $-1/N$  in parenthesis emerges due to  $q = 0, N/2$ . Long-time average of correlation function for  $n \neq 0$  can be calculated analogously. In the specific case  $\gamma = 0$  the result (B-10) coincides with the expression obtained in [7].

## C Group velocity of spin waves

In the present section we consider  $h \geq 0$ ,  $\gamma \in [0, 1]$ . Group velocity of spin waves reads

$$v(\varphi; h, \gamma) = (h - (1 - \gamma^2) \cos \varphi) \sin \varphi / E(\varphi; h, \gamma). \quad (\text{C-1})$$



We are interested mainly in the *maximal* velocity for given values of parameters  $h$  and  $\gamma$  :

$$V(h, \gamma) \equiv \sup_{\varphi} v(\varphi; h, \gamma) = v(\varphi_0; h, \gamma), \quad (\text{C-2})$$

where  $\varphi_0$  is the supremum point. Due to the symmetry of  $E(\varphi)$  we can consider  $\varphi \geq 0$  without loss of generality. Extremum condition  $\partial_{\varphi} v|_{\varphi_0} = 0$  leads to the fourth degree polynomial equation

$$P(z) \equiv (1-b)^2 z^4 - 3h(1-b)z^3 + (2b(1-b) + h^2(3-2b))z^2 - h(h^2+b)z - b(1-b) + h^2b = 0 \quad (\text{C-3})$$

with  $z = \cos \varphi_0$  and  $b \equiv \gamma^2$ . We are interested in the real roots of this equation which lie in the interval  $[-1, 1]$ . Let us show that there is only one such root whenever  $h \geq 1$  (this fact is important for the application of the method of the steepest descent, see Appendix D). In this case the above equation implies that  $z \geq 0$ , therefore in fact we have to consider the interval  $[0, 1]$ . Since  $P(0) > 0$ ,  $P(1) < 0$  and  $P(+\infty) = +\infty$ , we could have 1, 2 or 3 roots in  $[0, 1]$ . If there were 2 or 3 roots of  $P = 0$  in the considered interval, then the equation  $P' = 0$  would have 2 roots in  $[0, 1]$ . However the latter equation has no more than 1 root in the considered interval ( $z = \frac{h}{4(1-b)}$ ). Thus equation (C-3) has exactly 1 root in the interval  $[0, 1]$  for  $h \geq 1$ .

Let us now consider several important special cases.

**I.**  $\gamma = 0$ . In this case  $\varphi_0 = \pi/2$ ,  $V = 1$ .

**II.**  $\gamma = 1$ . In this case

$$\cos \varphi_0 = \begin{cases} h, & h \leq 1 \\ h^{-1}, & h > 1, \end{cases} \quad (\text{C-4})$$

and

$$V = \begin{cases} h, & h \leq 1 \\ 1, & h > 1, \end{cases} \quad (\text{C-5})$$

**III.**  $h = 0$ . In this case  $\cos \varphi_0 = -\sqrt{\frac{\gamma}{1+\gamma}}$ ,  $V = 1 - \gamma$ .

**IV.**  $h = 1$ . This is an especially interesting case as it corresponds to the quantum phase transition. Velocity  $v(\varphi)$  has a step at  $\varphi = 0$ , step height being equal to  $2\gamma$ . Eq. (C-3) is simplified to

$$(z-1)^2 ((b-1)^2 z^2 + (2b^2 - b - 1)z + b^2) = 0. \quad (\text{C-6})$$

One should distinguish two cases.

**IV a.**  $b \in [3/4, 1]$ . In this case the only root that satisfy  $|z| \leq 1$  is  $z = 1$ . Thus  $\varphi_0 = 0$ ,  $V = \gamma$ .

**IV b.**  $b \in [0, 3/4)$ . In this case  $\cos \varphi_0 = \frac{2b+1-\sqrt{4b+1}}{2(1-b)}$  from which one can easily write down an expression for  $V$  which appears to be somewhat bulky. One can also find a *minimal* value of  $V$  with respect to  $\gamma$  :

$$\inf_{\gamma \in [0, 1]} V(1, \gamma) = V(1, \sqrt{2 - \sqrt{2}}) = 2(\sqrt{2} - 1) = 0.828427... \quad (\text{C-7})$$

In what follows we show that this is the minimal value of  $V$  in the whole region  $h \geq 1, \gamma \in [0, 1]$ .

**V.**  $h \rightarrow \infty$ . In this case  $\varphi_0 \rightarrow 0$ ,  $V \rightarrow 1$ .

Let us investigate how  $V(h, \gamma)$  varies with  $h$ . The derivative over  $h$  has a rather simple form:

$$\partial_h V(h, \gamma) = b(1 - h \cos \varphi_0) \sin \varphi_0 / E^3(\varphi_0; h, \gamma). \quad (\text{C-8})$$

To calculate it we used that  $\partial_h V(h, \gamma) = \partial_h v(\varphi_0; h, \gamma)$  due to the equation  $\partial_\varphi v(\varphi_0; h, \gamma) = 0$ . The stationary points of  $V(h, \gamma)$  with respect to  $h$  are given by  $\partial_h V = 0$  which leads to  $\cos \varphi_0 = 1/h$ . We plug the latter equality into eq. (C-3) and obtain

$$(1 - \gamma^2)(1 - z^2)^2(1 - (1 - \gamma^2)z^2) = 0. \quad (\text{C-9})$$

The only roots that satisfy  $|z| \leq 1$  are  $z = \pm 1$  which correspond to  $h = 1$ . This point is not extremal because  $V(0, \gamma) \leq V(1, \gamma) \leq V(+\infty, \gamma)$ . Thus for any fixed  $\gamma$  maximal group velocity  $V(h, \gamma)$  monotonically grows with  $h$  from  $1 - \gamma$  at  $h = 0$  to 1 as  $h \rightarrow \infty$ . As a consequence, if one considers only  $h \geq 1$ , than the minimal value of  $V$  is given by eq. (C-7).

## D Asymptotic expressions

Here we consider in detail asymptotic expressions for spectral functions  $A_j(t)$  and  $B_j(t)$ . Let us explore domains in which  $E(\varphi)$  is an univalent analytical function. The branch points of this function are found from the equation  $(h - \cos \varphi)^2 + (\gamma \sin \varphi)^2 = 0$ . For  $h^2 > 1 - \gamma^2$  its solutions are  $\varphi_{br\pm}$  and  $\varphi_{br\pm}^*$ , where

$$\varphi_{br\pm} = 2\pi k + i \cdot \operatorname{arccosh} \left( \frac{h \pm \gamma \sqrt{h^2 - (1 - \gamma^2)}}{1 - \gamma^2} \right), \quad k \in Z. \quad (\text{D-1})$$

The domain where  $E(\varphi)$  remains univalent analytical function is the hole complex plane without row of branch cuts from  $\varphi_{br-}$  to  $\varphi_{br+}$  in the  $\operatorname{Im}(\varphi) > 0$  half-plane and row of branch cuts from  $\varphi_{br-}^*$  to  $\varphi_{br+}^*$  in the  $\operatorname{Im}(\varphi) < 0$  half-plane. It is important that  $\operatorname{Im}(E(\varphi))$  is positive in I and III quadrants and negative in II and IV quadrants. Functions  $E(\varphi)$ ,  $\varepsilon(\varphi)$ ,  $\exp[-ijN\varphi]$ , as well as integrands in eq.(13), are  $2\pi$  periodic functions of  $\operatorname{Re}(\varphi)$ . Thus we consider the strip  $\operatorname{Re}(\varphi) \in (-\pi; \pi]$ .

In order to use the method of the steepest descent for the integrals in eq.(13) we have to find saddle points for functions

$$f_{Aj}(\varphi) \equiv iE(\varphi)t - ijN\varphi, \quad f_{Bj}(\varphi) \equiv iE(\varphi)t - ijN\varphi + \ln \frac{\varepsilon(\varphi)}{E(\varphi)}. \quad (\text{D-2})$$

The saddle points are defined by the equations

$$E't - jN = 0, \quad \text{and} \quad iE't - ijN + \left( \ln \frac{\varepsilon}{E} \right)' = 0 \quad (\text{D-3})$$

correspondingly.

## D.1 Asymptotics for spectral functions of zero order

Let us first consider spectral functions of zero order,  $A_0(t)$  and  $B_0(t)$ . There are four saddle points in the strip  $\text{Re}(\varphi) \in (-\pi; \pi]$  which for  $A_0$  read

$$\varphi_1 = 0, \quad \varphi_2 = \pi, \quad \varphi_3 = -i \cdot \text{arccosh} \frac{h}{1 - \gamma^2}, \quad \varphi_4 = +i \cdot \text{arccosh} \frac{h}{1 - \gamma^2}. \quad (\text{D-4})$$

For  $B_0$  we have exactly the same points  $\varphi_1^B = \varphi_1$ ,  $\varphi_2^B = \varphi_2$  and slightly (for  $t \gg 1$ ) shifted points  $\varphi_3^B$  and  $\varphi_4^B$ :

$$\varphi_{3,4}^B = \mp i \cdot \text{arccosh} \left( \frac{h}{1 - \gamma^2} + c_{3,4} \cdot \frac{1}{t} + O\left(\frac{1}{t^2}\right) \right) \quad (\text{D-5})$$

One can find  $c_{3,4}$  by substituting  $\varphi_{3,4}^B = \varphi_{3,4} + \Delta \varphi$  in the second equation in (D-3). Note that if in the  $(c_{3,4} \cdot t^{-1})$ -vicinity of  $\varphi_{3,4}$  the series for  $E(\varphi)$  is convergent, then the difference between  $\varphi_3$  and  $\varphi_{3,4}^B$  is of order of  $t^{-1}$ .

Let us define the following parameter:

$$\epsilon \equiv h - 1. \quad (\text{D-6})$$

For large enough  $\epsilon$  we can find asymptotics in the case  $t \gg \max\{\epsilon^{-1}, 1\}$  in a straightforward way. Indeed, we can transform the integration path from our initial  $C_0$  (integration along  $\text{Re}(\varphi) = 0$  from  $\varphi = -\pi$  to  $\varphi = \pi$ ) to the path  $\tilde{C}_1$  which goes through I and III quadrant, where  $\text{Im}(E) > 0$ , and through saddle points  $\varphi_1 = 0$  and  $\varphi_2 = \pi$  (see figure (8), left). Then we immediately have

$$\begin{aligned} A_0(t) &\simeq \sqrt{\frac{1}{2\pi t}} \left( a_{0-} \cos((h-1)t + \frac{\pi}{4}) + a_{0+} \cos((h+1)t - \frac{\pi}{4}) + O\left(\frac{1}{t}\right) \right), \\ B_0(t) &\simeq \sqrt{\frac{1}{2\pi t}} \left( a_{0-} \sin((h-1)t + \frac{\pi}{4}) + a_{0+} \sin((h+1)t - \frac{\pi}{4}) + O\left(\frac{1}{t}\right) \right), \end{aligned} \quad (\text{D-7})$$

where

$$a_{0\pm} = \sqrt{\frac{h \pm 1}{h \pm (1 - \gamma^2)}}$$

and we take into account that  $\varepsilon(0)E^{-1}(0) = \varepsilon(\pi)E^{-1}(\pi) = 1$ . Region of applicability for large enough  $\epsilon$  is given by  $t \gg 1$ , and for  $\epsilon \rightarrow 0$  we have  $t > 2\epsilon^{-1} \ln \frac{1}{\Delta}$  where  $\Delta$  stays for the value of an error. Under these conditions we have the following approximation for  $t < t_{\text{th}}$ :

$$g_0^{zz}(t) \simeq \frac{1}{2\pi t} \cdot ((a_{0+} - a_{0-})^2 + 4a_{0+}a_{0-} \cos^2(t - \frac{\pi}{4})). \quad (\text{D-8})$$

Numerical evolution shows an excellent coincidence with the exact solution in the region  $1 \ll t < t_{\text{th}}$ . Note that this expression becomes asymptotic for  $J_0^2(t)$  in the case  $\gamma = 0$  (XX chain) which is in accordance with eq. (17).

Let us consider the case of such small  $\epsilon$  that  $\epsilon \ll \gamma$  and  $\epsilon \ll (t)^{-1}$ . Since we are interested in the dynamics on time scale of order of  $t_{\text{th}}$  or larger, the latter condition in fact implies  $\epsilon \ll N^{-1} \ll 1$ . Now we cannot integrate over the contour  $\tilde{C}_1$  due to the small convergence radius of the series in the vicinity of  $\varphi_1 = 0$  (note however that the

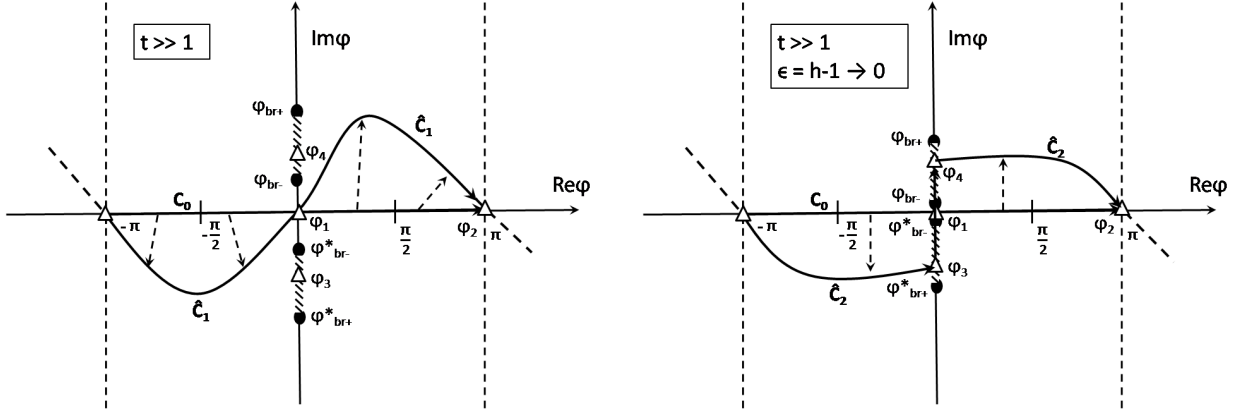


Figure 8: Integration paths for  $A_0, B_0$  in the case  $t \gg 1, t \gg \epsilon^{-1}$  (left) and in the case  $\epsilon^{-1} \gg t \gg 1, \gamma \gg \epsilon$  (right). Empty triangles correspond to saddle points, filled circles – to branch points of  $E(\varphi)$ .

contribution from the saddle point  $\varphi_2 = \pi$  remains intact). Therefore we use another integration path,  $\tilde{C}_2$  (see fig. (8)), which goes through saddle points  $-\pi, \varphi_3, \varphi_1, \varphi_4$  and ends up in  $\varphi_2 = \pi$ . Consider integration path from  $\varphi_3$  to  $\varphi_4$ . Integration over branch cuts does not contribute to  $A_j, B_j$  (this statement is true for spectral functions of all orders). This is because  $\text{Re}(E(\varphi)) = 0$  on the branch cuts, and therefore

$$\text{Re} \int_{\text{cut}} e^{itE(\varphi) - in\varphi} d\varphi = \text{Im} \int_{\text{cut}} \frac{\varepsilon(\varphi)}{E(\varphi)} e^{itE(\varphi) - in\varphi} d\varphi = 0. \quad (\text{D-9})$$

For small  $\epsilon$  branch points can be expanded as  $\varphi_{br-}, \varphi_{br-}^* = \pm i \cdot \epsilon \gamma^{-1} + O(\epsilon^2 \gamma^{-2})$ . At the segment  $[\varphi_{br-}^*, \varphi_{br-}]$  functions  $E(\varphi)$  and  $\varepsilon(\varphi)$  are real-valued, and  $E(\varphi) < \sqrt{2}\epsilon, \varepsilon(\varphi)E^{-1}(\varphi) = 1 + O(\epsilon)$ , therefore

$$\text{Re} \int_{\varphi_{br-}^*}^{\varphi_{br-}} e^{itE(\varphi)} d\varphi < (\sqrt{2}\gamma^{-1}\epsilon + O(\epsilon^2\gamma^{-2})) \cdot \min\{\epsilon t, 1\}, \quad (\text{D-10})$$

$$\text{Im} \int_{\varphi_{br-}^*}^{\varphi_{br-}} \frac{\varepsilon(\varphi)}{E(\varphi)} e^{itE(\varphi)} d\varphi = \gamma^{-1}\epsilon + O(\epsilon^2\gamma^{-2}).$$

Combining these results with contributions from saddle points  $\varphi_2, \varphi_3, \varphi_4$ , one obtains

$$A_0(t) \simeq \sqrt{\frac{1}{2\pi(2-\gamma^2)t}} \left( \sqrt{2} \cos(2t - \frac{\pi}{4}) + (1-\gamma^2)^{\frac{1}{4}} \exp[-\frac{\gamma^2}{\sqrt{1-\gamma^2}}t] + O(\frac{1}{t}) + O(\epsilon\gamma^{-1}) \right). \quad (\text{D-11})$$

For  $B_0$ , keeping in mind (D-5), one obtains

$$B_0(t) \simeq \sqrt{\frac{1}{2\pi(2-\gamma^2)t}} \left( \sqrt{2} \sin(2t - \frac{\pi}{4}) \right) \quad (\text{D-12})$$

$$+(1 - \gamma^2)^{-\frac{1}{4}} \exp\left[-\frac{\gamma^2}{\sqrt{1 - \gamma^2}}t\right] + O\left(\frac{1}{t}\right) + O(\epsilon\gamma^{-1})\Bigg).$$

Region of applicability for these asymptotics is limited by the condition that  $\exp[-\frac{1}{2}|E''(\varphi_3)|R^2]$  must be small enough (here  $R$  is the radius of convergence for  $E(\varphi)$  near  $\varphi_{3,4}$ ). We have  $R = |\varphi_3 - \varphi_{br+}| \simeq (2 - \sqrt{2})\gamma$  for small  $\gamma$ . Thus we get the following condition of applicability for the above asymptotic:

$$t > (2 - \sqrt{2})^{-2}\gamma^{-2} \ln\left(\frac{1}{\Delta}\right), \quad (\text{D-13})$$

where  $\Delta$  is the order of the relative error. Under this condition we can neglect the term  $\exp[-\gamma^2(1 - \gamma^2)^{-\frac{1}{2}}t]$  in (D-11) and (D-12). Numerical evaluation shows excellent coincidence of these asymptotics with the exact values of  $A_0$  and  $B_0$  in the case  $\gamma \ll 1$ ,  $t \gg 1$ . Moreover, these expressions exactly coincide with asymptotic forms for Bessel functions in (15) in the case  $\gamma = 0$ ,  $h = 1$  which is not obvious from our derivation method. With these remarks, we find

$$g_0^{zz}(t) = \frac{1}{\pi(2 - \gamma^2)t} \left( 1 + \frac{2 - \gamma^2}{2\sqrt{1 - \gamma^2}} \exp\left[-\frac{2\gamma^2}{\sqrt{1 - \gamma^2}}t\right] + 2\sqrt{\frac{2 - \gamma^2}{2\sqrt{(1 - \gamma^2)}}} \exp\left[-\frac{\gamma^2}{\sqrt{1 - \gamma^2}}t\right] \cos\left(2t - \frac{\pi}{4} - \arctan \frac{1}{\sqrt{1 - \gamma^2}}\right) \right), \quad (\text{D-14})$$

which gives us an excellent approximation for  $g_0^{zz}(t)$  in the case  $\epsilon \ll \gamma$ ,  $\epsilon \ll N^{-1}$ ,  $t < t_{\text{th}}$ . For not very small  $\gamma^2$  we can neglect exponential suppressed terms and obtain

$$g_0^{zz}(t) = \frac{1}{\pi(2 - \gamma^2)t}. \quad (\text{D-15})$$

## D.2 Asymptotics for spectral functions of non-zero order

For spectral functions of non-zero orders the situation is slightly more complicated. Again there are four saddle points in the strip  $\text{Re}(\varphi) \in (-\pi, \pi]$ , but now their positions *vary with time* (see fig. 9). Consider the function  $A_j$ ,  $j \geq 1$ . The corresponding saddle points satisfy the 4-degree polynomial equation on  $z = \cos \varphi$ :

$$(1 - \gamma^2)^2 z^4 - 2h(1 - \gamma^2)z^3 + [(h^2 - (1 - \gamma^2)^2) + \zeta(1 - \gamma^2)]z^2 + [h(1 - \gamma^2) - 2\zeta h]z - h^2 + \zeta(h^2 + \gamma^2) = 0, \quad (\text{D-16})$$

where  $\zeta \equiv (Nj)^2(t)^{-2}$ . This equation viewed as the equation on  $\varphi$  gives eight solutions in the strip  $\text{Re}(\varphi) \in (-\pi, \pi]$ . Four of them are relevant (i.e. are solutions of eq. (D-3)) and other four are irrelevant (are solutions of the equation  $-E't - jN = 0$ ). Since  $E'(\varphi)$  takes all possible real values on the each branch cut, one pair of saddle points,  $\varphi_3$  and  $\varphi_4$ , lies on two brunch cuts symmetrically with respect to the real axis, analogous to the  $j = 0$  case.

Let us consider the positions of two other saddle points,  $\varphi_1$  and  $\varphi_2$ , especially their evolution with time. The definition of the threshold time implies that for  $t < jt_{\text{th}}$  eq.(D-3) has no real roots. Thus  $\varphi_1$  and  $\varphi_2$  are complex. In fact they are complex conjugate

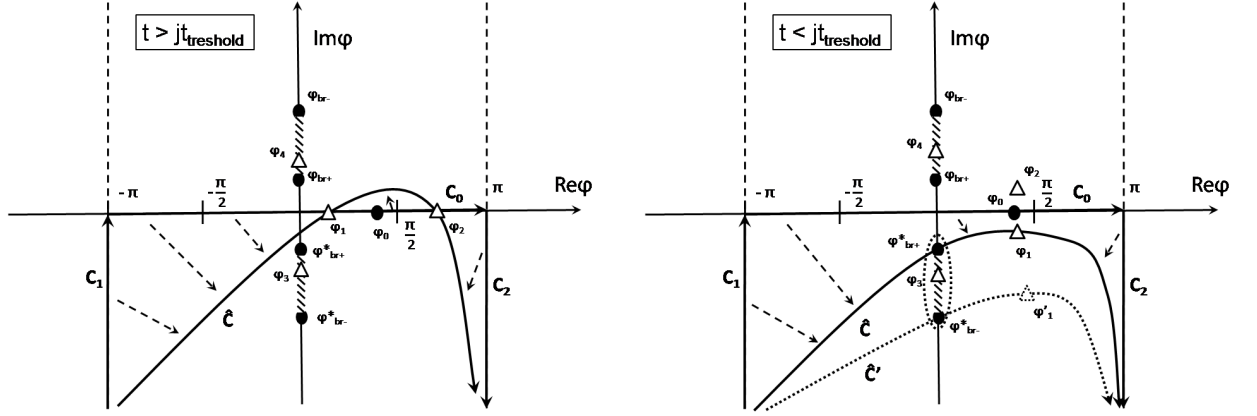


Figure 9: Integration paths for  $A_j$ ,  $B_j$  in the case  $t > jt_{\text{th}}$  (left) and in the case  $t < jt_{\text{th}}$  (right). Empty triangles correspond to saddle points, filled circles – to branch points and to the point  $\varphi_0$  which satisfies  $E(\varphi_0)'' = 0$ .

to each other. When time goes on they both approach  $\varphi_0$  which lies on the real axis, and eventually merge at  $t = jt_{\text{th}}$ :  $\varphi_1(jt_{\text{th}}) = \varphi_2(jt_{\text{th}}) = \varphi_0$ . For  $t > jt_{\text{th}}$   $\varphi_1$  and  $\varphi_2$  lie on the real axis and move apart from  $\varphi_0$  and from each other, approaching 0 and  $\pi$  correspondingly as  $t \rightarrow \infty$ .

### D.2.1 Asymptotics for $t > jt_{\text{th}}$

To start with, we warn the reader that we do not provide a strict mathematical proof that the suitable integration path exists which goes through the chosen saddle points in all presented cases. However, the existing of these paths looks quite natural in all cases and, moreover, corresponding asymptotic expressions show excellent coincidence with numerical evolutions. Strict mathematical proof is postponed for further work.

With this warning made, let us turn to the case  $t > jt_{\text{th}}$ . We start from the case of non-small  $\epsilon$  and we assume that  $\varphi_1$  and  $\varphi_2$  are situated far enough from each other, so that we can neglect their mutual influence in the asymptotics. The conditions under which this assumption is fulfilled are considered in what follows.

Note that we can integrate along the path  $C_1 \cup C_0 \cup C_2$ , where  $C_0$  is the original path,  $C_1$  starts from  $\varphi = -\pi - i\infty$  and goes to  $\varphi = -\pi$  along  $\text{Re}\varphi = \text{const} = -\pi$ ,  $C_2$  starts from  $\varphi = \pi$  and goes to  $\varphi = \pi - i\infty$  along  $\text{Re}\varphi = \text{const} = \pi$  (see fig. 9). Since  $f_{A,B_j}(x + iy)$  are  $2\pi$  periodic functions of  $x$ , the value of the integral along the new path is exactly the same as along  $C_0$ . Now we transform the path  $C_1 \cup C_0 \cup C_2$  to the path  $\hat{C}$  which starts from  $\varphi = -\pi - i\infty$ , goes through saddle points  $\varphi_1$  and  $\varphi_2$  and ends at  $\varphi = \pi - i\infty$  (see fig. 9, left). There are two topological different possible integration paths  $\hat{C}$ : the first one goes above the branch cut, while the second one - under the cut. In the latter case according to the Cauchy theorem we have to subtract the integral over the branch cut. However as was discussed above this integral does not contribute to  $A_j$  and  $B_j$  (see eq.(D-9)).

Now we can proceed to find asymptotic expressions as contribution from points  $\varphi_1$  and  $\varphi_2$ . Under all specified conditions, we immediately obtain eq. (24) for  $A_j$ . For  $B_j$ ,

using reasonings similar to those following eq. (D-5), we get eq. (25).

Let us now investigate the range of applicability of eqs. (24), (25). Firstly we consider in what cases we can use the standard approximation for contribution of saddle points under the assumption that radius of convergence for corresponding series is large enough. In this case the derived approximation may deviate from the exact expression for two reasons: small value of  $|E(\varphi_{1,2})''|$  and interception of contributions for  $\varphi_1$  and  $\varphi_2$  due to their close relative position. These two features can appear only for small times after  $jt_{\text{th}}$ . Let us give more precise estimation without detail explanations. If  $\delta t \equiv t - jt_{\text{th}} > 0$ , then it has to be  $\frac{\delta t}{t_{\text{th}}} > \sqrt[3]{\frac{j}{2 \cdot r \cdot N^2}}$ , where  $r \equiv \frac{E(\varphi_0)}{|E'''(\varphi_0)|}$  is quantity of order of 1 for the vast majority of the Hamiltonian parameter space. One can see that these asymptotic approximations for spectral functions of order  $j$  become accurate starting from time close to  $jt_{\text{th}}$ .

Now let us investigate in what cases series does not converge in large enough circle for some saddle point. We have to explore small enough  $\epsilon$ , at least  $\epsilon^{-1} \gg t$ . Since for spectral function of order  $j$  we are interested in  $t > jt_{\text{th}}$ , it is useful to consider  $\epsilon^{-1} \gg jN$ . Firstly we define the position of  $\varphi_0$  :

$$\varphi_0 = \arccos\left(\frac{2\gamma^2 + 1 - \sqrt{4\gamma^2 + 1}}{2(1 - \gamma^2)}\right) + O(\epsilon), \quad \gamma^2 \leq \frac{3}{4}, \quad (\text{D-17})$$

$$\varphi_0 = \frac{2^{\frac{1}{2}} \epsilon^{\frac{1}{2}}}{(4\gamma^2 - 3)^{\frac{1}{4}}} + O(\epsilon), \quad \gamma^2 > \frac{3}{4}.$$

Let us consider the case  $\gamma^2 < \frac{3}{4}$ . For times which satisfy  $jt_{\text{th}} < t < \tilde{jt}_{\text{th}} = jN\gamma^{-1} + O(\epsilon)$  there is no point  $\varphi_1$  near  $\varphi = 0$ , and the derived asymptotic expressions (24), (25) are valid. If  $t > \tilde{t}_{\text{th}}$  one obtains

$$\varphi_1 = \frac{\epsilon}{\gamma \sqrt{\frac{\gamma^2 t^2}{j^2 N^2} - 1}} + O(\epsilon^2), \quad t > \tilde{jt}_{\text{th}} = j \frac{N}{\gamma} + O(\epsilon). \quad (\text{D-18})$$

Thus for  $t \ll \epsilon^{-1}$  we cannot use the above derived approximations because  $\varphi_1$  is situated close to  $\varphi_{br-}$  and the radius of convergence  $R = \sqrt{\epsilon^2 \gamma^2 + \varphi_1^2}$  is very small,  $|E''(\varphi_1)|tR^2 < 1$ , thus we cannot use the method of the steepest descent for  $\varphi_1$  (we assume here  $\gamma \gg \epsilon$ ). Instead we can proceed analogously to the case of spectral functions of zero order. Namely, we move the integration path in order to go through saddle points  $\varphi_3$  and  $\varphi_4$  and neglect the value of integral between  $\varphi_{br-}^*$  and  $\varphi_{br-}$  as we have done in (D-7). The difference from the case of  $A_0$  and  $B_0$  is that now we can neglect exponentially suppressed contribution from  $\varphi_3$ , but contribution from  $\varphi_4$  may be not small for some portion of time. Numerical evaluation shows that for  $N \gg 1$  the contribution from  $\varphi_4$  is exponentially suppressed at a timescale  $\sim \tilde{t}_{\text{th}}$ . Summarizing, for time  $t > \tilde{t}_{\text{th}}$  we obtain

$$A_j(t) \simeq \frac{1}{\sqrt{2\pi t}} \left( \frac{1}{2} \sqrt{\frac{1}{|E''(\varphi_4)|}} \exp[-t(-iE(\varphi_4 + 0)) + jN(-i\varphi_4)] \right. \\ \left. + \sqrt{\frac{1}{|E''(\varphi_2)|}} \cos(tE(\varphi_2) - jN\varphi_2 - \frac{\pi}{4}) + O\left(\frac{1}{t}\right) \right), \quad (\text{D-19})$$

where one should remind that  $-iE(\varphi_4 + 0) > 0$ ,  $(-i\varphi_4) > 0$ . Factor  $\frac{1}{2}$  is due to the fact that we have to take only one half of contribution from  $\varphi_4$ . Analogously one obtains

$$B_j(t) \simeq \frac{1}{\sqrt{2\pi t}} \left( \frac{1}{2} \frac{\varepsilon(\varphi_4)}{(-iE(\varphi_4 + 0))} \sqrt{\frac{1}{|E''(\varphi_4)|}} \exp[-t(-iE(\varphi_4 + 0)) + jN(-i\varphi_4)] \right. \\ \left. + \frac{\varepsilon(\varphi_2)}{E(\varphi_2)} \sqrt{\frac{1}{|E''(\varphi_2)|}} \sin(tE(\varphi_2) - jN\varphi_2 - \frac{\pi}{4}) + O(\frac{1}{t}) \right). \quad (\text{D-20})$$

The only case we do not investigate here is  $\gamma \leq \epsilon \ll 1$ . We leave it for future work.

If  $\gamma^2 \geq \frac{3}{4}$ , then  $\varphi_0$  is situated in the vicinity of  $\varphi = 0$ , which leads to  $t_{\text{th}} = \tilde{t}_{\text{th}} = N\gamma^{-1} + O(\epsilon)$ . Therefore asymptotic expressions (D-19), (D-20) are valid starting from time  $t$  for which  $\varphi_2$  is situated far enough from  $\varphi = 0$  (the corresponding condition reads  $\frac{1}{2}|E''(\varphi_2)|t\varphi_2^2 \gg 1$ ). For times in the vicinity of  $jt_{\text{th}}$  another approximation should be used, see Sec. D.2.3.

### D.2.2 Asymptotics for $t < jt_{\text{th}}$

When  $t < jt_{\text{th}}$  the path of integration should not go through the I quadrant, since for all values of  $x \in (-\pi; \pi)$   $\partial_y \text{Re}(iEt - in\varphi) > 0$  (remind that  $\varphi = x + iy$ ). We shift our integration path to  $\tilde{C}$  or  $\tilde{C}'$  (see figure (9)) and obtain asymptotics from the contribution from only one saddle point,  $\varphi_1$ . For large enough  $|\delta t|$ , where  $\delta t \equiv t - jt_{\text{th}} < 0$ , we have

$$A_j(t) \simeq \sqrt{\frac{1}{2\pi|E''(\varphi_1)|t}} \cos(E(\varphi_1)t - jN\varphi_1 + \sigma(\varphi_1)), \quad (\text{D-21})$$

where  $\sigma(\varphi_1)$  is the angle between the path and the line  $\text{Im}f_{A_j} = \text{const}$ . Let us evaluate  $\varphi_1$  approximately for  $t \lesssim jt_{\text{th}}$  such that  $t^{-1}\delta t \ll 1$ . If  $E_0''' \equiv E'''(\varphi_0) \neq 0$ , then

$$\varphi_1 = \varphi_0 - i\eta + \frac{1}{6} \frac{E_0^{(IV)}}{E_0'''} \eta^2 + i \left( \frac{5}{72} \left( \frac{E_0^{(IV)}}{E_0'''} \right)^2 - \frac{1}{24} E_0^{(V)} \right) \eta^3 + O(\eta^4) + iO(\eta^5), \quad (\text{D-22})$$

where

$$\eta \equiv \sqrt{-\frac{2N\delta t}{|E_0'''|t t_{\text{th}}}} = \sqrt{-2r \frac{\delta t}{t}}, \quad r \equiv \frac{E_0'}{|E_0''|}$$

Up to the first order in  $\delta t \cdot t^{-1} \simeq \delta t \cdot j^{-1}t_{\text{th}}^{-1}$  one obtains

$$A_j(t) \simeq \frac{r^{\frac{1}{4}}(jN)^{\frac{1}{2}}}{2^{\frac{3}{4}}\pi^{\frac{1}{2}}} \left( \frac{-\delta t}{jt_{\text{th}}} \right)^{-\frac{1}{4}} \exp\left[ \frac{-2\sqrt{2}r}{3} jN \left( \frac{-\delta t}{jt_{\text{th}}} \right)^{\frac{3}{2}} + O\left( \left( \frac{-\delta t}{jt_{\text{th}}} \right)^{\frac{5}{2}} \right) \right] \cos(E(\varphi_0)t - jN\varphi_0) \\ + O\left( \left( \frac{-\delta t}{jt_{\text{th}}} \right)^{\frac{3}{4}} \right). \quad (\text{D-23})$$

This expressions gives only the order of suppression; if one is interesting in more precise expression, he has to directly solve eq.(D-3) to find an exact value of  $\varphi_1$  and substitute



it in the general formula (D-21). This formula (and approximation (D-23)) is valid until we can neglect the term  $\frac{1}{6}E'''(\varphi_1)(\Delta\varphi)^3$  in comparison with  $\frac{1}{2}E''(\varphi_1)(\Delta\varphi)^2$  in series expansion near  $\varphi_1$ . This leads to the condition  $jN(\frac{\delta t}{jt_{\text{th}}})^{\frac{3}{2}} \gg 1$ . In the opposite case,  $jN(\frac{\delta t}{jt_{\text{th}}})^{\frac{3}{2}} \ll 1$ , eqs. (D-3) and (D-23) are not valid and the leading order contribution is given by the term  $\frac{1}{6}E'''(\varphi_1)(\Delta\varphi)^3$ , which leads to

$$A_j(t) \simeq \frac{\Gamma(\frac{1}{3})r^{\frac{1}{3}}}{2^{\frac{2}{3}}3^{\frac{1}{6}}\pi j^{\frac{1}{3}}N^{\frac{1}{3}}} \cdot \left( \frac{|E(\varphi_0)'''|t_{\text{th}}}{|E(\varphi_1)'''|t} \right)^{\frac{1}{3}} \cdot \cos(E(\varphi_1)t - jN\varphi_1), \quad (\text{D-24})$$

where values of  $E(\varphi_1)$  and  $E(\varphi_1''')$  may be found according to eq. (D-22). Eqs. (D-24) and (D-23) become asymptotics for  $J_j(t)$  in the case of  $XX$  chain. If one wants to derive asymptotics valid in the region  $jN(\frac{\delta t}{jt_{\text{th}}})^{\frac{3}{2}} \sim 1$ , he has to calculate the integral through saddle point with proper path direction (here we use approximation (D-22) for saddle points),

$$I_{\text{saddle}}(t) \simeq \int \exp[-\frac{1}{2}\eta|E_0'''|tz^2 - \frac{i}{6}|E_0'''|tz^3]dz, \quad (\text{D-25})$$

and use the formula

$$A_j(t) \simeq \frac{1}{2\pi} I_{\text{saddle}}(t) \exp[\frac{-2\sqrt{2r}}{3}jN(\frac{-\delta t}{jt_{\text{th}}})^{\frac{3}{2}}] \cos(E(\varphi_0)t - jN\varphi_0). \quad (\text{D-26})$$

Eqs. (D-23) and (D-24) can be obtained from the above formula by neglecting the second summand in the exponent in (D-25) and by expansion of the integrand in eq.(D-25) in powers of  $\eta$ .

Let us turn to  $B_j$ . In order to describe its behavior in analogous way one should start from

$$B_j(t) \simeq \text{Im} \left( \sqrt{\frac{1}{2\pi|E''(\varphi_1)|t}} \frac{\varepsilon(\varphi_1)}{E(\varphi_1)} \exp[iE(\varphi_1)t - ijN\varphi_1 + i\sigma(\varphi_1)] \right) \quad (\text{D-27})$$

instead of (D-21). We do not describe in details  $B_j(t)$  because there is no simple approximation formula for (D-27) for all possible values of  $\cos(\varphi_0)$ . However the exponential suppression for  $B_j(t)$  has the same form as for  $A_j(t)$ , only the preexponential factor differs. This is because the suppression is determined by the exponent of the quantity  $-\text{Re}(-iE(\varphi_1)t + ijN\varphi_1)$  which is the same for  $B_j$  and  $A_j$  up to  $t^{-1}$ .

To conclude this subsection, the suppression of spectral functions  $A_j(t)$  and  $B_j(t)$  with  $\delta t = t - jt_{\text{th}} < 0$  with exponential precision reads

$$A_j(t) \sim B_j(t) \sim \exp[-\frac{2}{3}\sqrt{\frac{2E'(\varphi_0)}{|E'''(\varphi_0)|}}jN(\frac{-\delta t}{jt_{\text{th}}})^{\frac{3}{2}} + O((\frac{-\delta t}{jt_{\text{th}}})^{\frac{5}{2}})]. \quad (\text{D-28})$$

This is in accordance with a general result [13]. Here we assume that  $E'''(\varphi_0) \neq 0$ ; for very small  $E'''(\varphi_0)$  one has to take into account  $E^{(IV)}(\varphi_0)$  which leads to a slightly different law.

### D.2.3 Asymptotics for $t \simeq jt_{\text{th}}$

The considerations of the present subsection are less rigorous than in the previous ones. The only consequence, however, is that we do not completely control errors for derived approximations. Numerical calculations demonstrate that the latter are nevertheless rather accurate in a wide range of model parameters. For certain regions of the parameter space in which the derived approximations fail we are able to identify the reason and point out the way to overcome the difficulties.

Let us describe the method. When  $t \simeq t_{\text{th}}$  the saddle points are situated near  $\varphi_0$ . Integrand is a very fast oscillating function for all  $\varphi$  except  $\varphi \simeq \varphi_0$ . Thus the value of the integral is picked up on a small segment  $[\varphi_0 - \Delta\varphi; \varphi_0 + \Delta\varphi]$ ,  $\Delta\varphi > \frac{1}{2}(\varphi_2 - \varphi_1)$ . In order to estimate errors for this approximation, one has to make bulky calculations in the spirit of the above subsections. We avoid this in the present work.

In order to calculate the integral along the small segment, we expand  $E(\varphi)$  in the vicinity of  $\varphi_0$ . And the last approximation is to replace the interval of integration from  $[-\Delta\varphi, \Delta\varphi]$  to  $[-\infty; \infty]$ , where the integration variable is  $\mu \equiv \varphi - \varphi_0$ . The latter trick is justified because our new integrand oscillate as  $\sim \exp(i \cdot \text{const} \cdot \mu^3)$  when  $\mu \rightarrow \pm\infty$ . All these approximations are legitimate when the model parameters are such that  $\varphi_0$  is far enough from points of branching. Thus the approximation is valid for large enough  $\epsilon$  and all values of  $\gamma$  and for  $\epsilon \ll 1$  it is valid for  $\gamma^2 < \frac{3}{4}$ . Let us assume that  $E_0''' \equiv E'''(\varphi_0)$  is not very small. In this case one can consider power expansion of  $E(\varphi)$  up to  $(\varphi - \varphi_0)^3$  and neglect terms  $\sim O((\varphi - \varphi_0)^4)$ . Thus for  $t \simeq jt_{\text{th}}$  one gets

$$\begin{aligned} A_j(t) &= \frac{1}{2\pi} \int_{-\pi}^{\pi} \cos(Et - jN\varphi) d\varphi \simeq \frac{1}{2\pi} \int_{-\Delta\varphi}^{\Delta\varphi} \cos(E_0 t - jN\varphi_0 + (E_0' t - jN)\mu - \frac{1}{6}|E_0'''|t\mu^3) d\mu \\ &\simeq \left( \frac{2}{|E_0'''|t} \right)^{\frac{1}{3}} \frac{1}{2\pi} \int_{-\infty}^{\infty} \cos[(E_0 t - jN\varphi_0) - \frac{t - jt_{\text{th}}}{t_{\text{th}}} N \left( \frac{2}{|E_0'''|t} \right)^{\frac{1}{3}} \xi + \frac{1}{3}\xi^3] d\xi. \end{aligned} \quad (\text{D-29})$$

Here all functions  $f$  with subindex 0 should be understood as  $f_0 \equiv f(\varphi_0)$ . The above integral is a well-known Airy function of the first kind:

$$\text{Ai}(x) \equiv \frac{1}{\pi} \int_0^{\infty} \cos\left(\frac{\xi^3}{3} + x\xi\right) d\xi \quad (\text{D-30})$$

Thus we get eq. (26) (with analogously reasonings for  $B_j$ ).

Let us investigate now the case  $h = 1$ ,  $\gamma^2 > \frac{3}{4}$  (we do not investigate here the case of small, but non-zero  $\epsilon = h - 1 \ll 1$ ). For  $h = 1$ ,  $\gamma^2 > \frac{3}{4}$  we cannot use formula (D-29), since  $\varphi_0 = \varphi_{br-} = \varphi_{br-}^* = 0$ . But we can argue that the main contribution for  $A_j$  is picked up on the segment  $[0, \Delta\varphi]$ , since only on this segment oscillation frequency is not very large (note that for  $[-\Delta\varphi, 0]$  the frequency is large; this is due to the discontinuity of the group velocity at  $\varphi = 0$ ). If we somehow expand  $E(\varphi)$  on  $[0, \Delta\varphi]$ , we can obtain a good approximation. Consider  $-E(\varphi)$  on a complex plain. If we have values for  $E(\varphi)$  on the segment  $\varphi \in [0, \pi]$  fixed, we can make analytical continuation to  $\text{Re}(\varphi) \in [-\pi, 0]$  in two different ways: with the branch cut:  $\text{Re}(\varphi_{\text{branch cut}}) = 0$ ,  $\text{Im}(\varphi_{\text{branch cut}}) \in [-\varphi_{br+}^*, \varphi_{br+}]$  or with the branch cut:  $\text{Re}(\varphi_{\text{branch cut}}) = 0$ ,  $\text{Im}(\varphi_{\text{branch cut}}) \in [-\infty, -\varphi_{br+}^*] \cup [\varphi_{br+}, \infty]$ . In the first case we have our original function  $E(\varphi)$  in the segment  $\varphi \in [-\pi, 0]$ . In the

second case we have some new function  $\tilde{E}(\varphi)$  which does not coincide with  $E(\varphi)$  in this segment. But in the latter case we can use power expansion for  $\tilde{E}(\varphi)$  in the circle with radius  $R = |\varphi_{br+}|$ :

$$\tilde{E}(\varphi) = \gamma\varphi + \frac{3-4\gamma^2}{24\gamma}\varphi^3 + \frac{16\gamma^4-15}{1920\gamma^3}\varphi^5 + O(\varphi^7). \quad (\text{D-31})$$

Analogously to (D-29) one obtains

$$A_j(t) \simeq \frac{1}{2\pi} \int_0^\infty \cos[(\gamma t - jN)\varphi + \frac{3-4\gamma^2}{24\gamma}t\varphi^3 + \frac{16\gamma^4-15}{1920\gamma^3}t\varphi^5] d\varphi. \quad (\text{D-32})$$

If one can neglect the term  $\sim \varphi^5$  (i.e. if  $\gamma^2 - \frac{3}{4}$  is large enough), he gets

$$A_j(t) \simeq \frac{1}{2} \left( \frac{2\gamma}{(\gamma^2 - \frac{3}{4})t} \right)^{\frac{1}{3}} \cdot \text{Ai} \left[ -(\gamma t - jN) \left( \frac{2\gamma}{(\gamma^2 - \frac{3}{4})t} \right)^{\frac{1}{3}} \right], \quad h=1, \gamma^2 > \frac{3}{4}. \quad (\text{D-33})$$

For  $B_j$  one uses power expansion  $\varepsilon(\varphi)E^{-1}(\varphi)$  in the vicinity of  $\varphi = 0$  to obtain

$$B_j(t) \simeq \frac{1}{4\gamma} \left( \frac{2\gamma}{(\gamma^2 - \frac{3}{4})t} \right)^{\frac{2}{3}} \cdot \text{Ai}' \left[ -(\gamma t - jN) \left( \frac{2\gamma}{(\gamma^2 - \frac{3}{4})t} \right)^{\frac{1}{3}} \right], \quad h=1, \gamma^2 > \frac{3}{4}, \quad (\text{D-34})$$

where prime stands for the derivative.

Let us consider the special case  $h=1, \gamma^2 = \frac{3}{4}$ . We have  $t_{\text{th}} = \frac{2}{\sqrt{3}}N$ . The term  $\sim \varphi^3$  in power expansion  $\tilde{E}(\varphi)$  is zero:  $\tilde{E}(\varphi) = \frac{\sqrt{3}}{2}\varphi - \frac{1}{120\sqrt{3}}\varphi^5$ . Let us introduce the function

$$\text{gAi}_n(x) \equiv \frac{1}{\pi} \int_0^\infty \cos\left(\frac{\xi^n}{n} + x\xi\right) d\xi \quad (\text{D-35})$$

Airy function of the first kind is a particular case of this function:  $\text{Ai}(x) = \text{gAi}_3(x)$ .  $\text{gAi}_n(x)$  for  $n > 3$  exhibits the same behavior as  $\text{Ai}(x)$ : for positive  $x$  it is exponentially decreasing, and for negative  $x$  it oscillates and goes to zero when  $x \rightarrow -\infty$ .  $A_j$  and  $B_j$  are expressed through this function and its derivative:

$$A_j(t) \simeq \frac{1}{2} \left( \frac{24\sqrt{3}}{t} \right)^{\frac{1}{5}} \cdot \text{gAi}_5 \left[ -\left( \frac{\sqrt{3}t}{2} - jN \right) \left( \frac{24\sqrt{3}}{t} \right)^{\frac{1}{5}} \right], \quad h=1, \gamma^2 = \frac{3}{4} \quad (\text{D-36})$$

$$B_j(t) \simeq \frac{1}{4\gamma} \left( \frac{24\sqrt{3}}{t} \right)^{\frac{2}{5}} \cdot \text{gAi}'_5 \left[ -\left( \frac{\sqrt{3}t}{2} - jN \right) \left( \frac{24\sqrt{3}}{t} \right)^{\frac{1}{5}} \right], \quad h=1, \gamma^2 = \frac{3}{4}$$

Note that rather small value of the coefficient of term  $\varphi^5$  in power expansion of  $\tilde{E}(\varphi)$  implies that these approximations work well for sufficiently large time ( $t \gg 24\sqrt{3}$ ). Analogously we require  $t \gg 2\gamma(\gamma^2 - \frac{3}{4})^{-1}$  in eqs. (D-33), (D-34). Note that if one wishes to investigate approximations which successfully describe  $A_j, B_j$  near threshold time in the region of parameter space  $h=1, \gamma^2 \simeq \frac{3}{4}$ , then one has to calculate integral (D-32) saving

both terms  $\sim \varphi^3$  and  $\sim \varphi^5$ . Therefore, in this case there is no such clear power law for time dependence of maximum value of spectral function as in (D-37).

Now let us discuss possible values of maximums for  $A_j$  and  $B_j$ . If  $jN$  is sufficiently large the positions of global maximums of  $A_j$  and  $B_j$  coincide with those for  $\text{Ai}(x)$  and  $\text{gAi}_5(x)$  :

$$\begin{aligned} \sup_t A_j(t) &\simeq \left( \frac{2}{|E_0'''|t} \right)^{\frac{1}{3}} \cdot a_3, \quad \text{for } h > 1; \text{ or } h = 1, \gamma^2 < \frac{3}{4} \\ \sup_t A_j(t) &\simeq \frac{1}{2} \left( \frac{2\gamma}{(\gamma^2 - \frac{3}{4})t} \right)^{\frac{1}{3}} \cdot a_3, \quad \text{for } h = 1, \gamma^2 > \frac{3}{4} \\ \sup_t A_j(t) &\simeq \frac{1}{2} \left( \frac{24\sqrt{3}}{t} \right)^{\frac{1}{5}} \cdot a_5, \quad \text{for } h = 1, \gamma^2 = \frac{3}{4} \end{aligned} \quad (\text{D-37})$$

Here  $a_3$  and  $a_5$  are global maximums of  $\text{Ai}(x)$  and  $\text{gAi}_5(x)$  ( $a_3 = 0,54\dots$ ,  $a_5 = 0.44\dots$ ) correspondingly. Without loss of precision one can replace  $t$  by  $jt_{\text{th}}$  in the above expressions. We do not present the analogous expressions for  $B_j(t)$  because positions of maximums of these functions obviously do not coincide with those for  $A_j$  (when  $A_j(t)$  achieves global maximum  $B_j(t)$  becomes zero). In the last two cases in eq. (D-37) it is  $A_j^2$  which gives the main contribution in  $g_0^{zz}(t)$  near  $t = jt_{\text{th}}$ . When  $h > 1$  or  $h = 1, \gamma^2 < \frac{3}{4}$  one has to investigate maximum of  $A_j(t)^2 + B_j(t)^2$  in order to find the leading contribution to  $g_0^{zz}(t)$ . This leads to

$$\begin{aligned} \text{Max}_{(\text{revival } j)}[g_0^{zz}(t)] &\simeq 4 \left( \frac{2}{|E_0'''|jt_{\text{th}}} \right)^{\frac{2}{3}} \cdot (1 + |\frac{\epsilon_0}{E_0} - 1|)a_3^2 \quad \text{for } h > 1; \text{ or } h = 1, \gamma^2 < \frac{3}{4}, \\ \text{Max}_{(\text{revival } j)}[g_0^{zz}(t)] &\simeq \left( \frac{2\gamma^2}{(\gamma^2 - \frac{3}{4})jN} \right)^{\frac{2}{3}} \cdot a_3^2, \quad \text{for } h = 1, \gamma^2 > \frac{3}{4}, \\ \text{Max}_{(\text{revival } j)}[g_0^{zz}(t)] &\simeq \left( \frac{36}{jN} \right)^{\frac{2}{5}} \cdot a_5^2, \quad \text{for } h = 1, \gamma^2 = \frac{3}{4}. \end{aligned} \quad (\text{D-38})$$

Note that this is a rather rude approximation, since interference terms may be large. Therefore these expressions work well only for large number of spins. Numerical evolution shows that the revivals are maximally pronounced for  $h = 1$  and  $\gamma^2$  slightly less then  $\frac{3}{4}$ . This may be expected on the basis of eq. (D-32).

Let us emphasize once more time that all the derived expressions can be derived with more rigor using integrals in the complex plain analogously to that was done in the previous subsections. We have not explored the whole parameter space. In particular, we have not considered the cases  $h = 1, \gamma^2 \simeq \frac{3}{4}$ ,  $\epsilon = h - 1 \ll 1, \epsilon \neq 0$ , or  $h > 1, E_0''' = 0$ . Some of the derived approximations work well only for large time and, correspondingly, large number of spins (for example,  $t \gg 24\sqrt{3}$  or  $t \gg 2\gamma(\gamma^2 - \frac{3}{4})^{-1}$ ). However, for a large region of parameter space these approximations work fairly well, and they provide an opportunity to investigate amplitudes of maximums in partial revivals, or at least the law of there decrease. For these reasons we decided to include in the paper these not completely rigorous calculations. The validity of formulae derived in the present subsection is justified by the fact that approximations (26) give the same result as the more rigorously derived eqs. (D-23) and (D-24) when the ranges of applicability overlap.

## References

- [1] D. Porras and J. I. Cirac. Effective quantum spin systems with trapped ions. *Phys. Rev. Lett.*, 92(20):207901, May 2004.
- [2] S. Bose. Quantum communication through an unmodulated spin chain. *Physical review letters*, 91(20):207901, 2003.
- [3] E. Lieb, T. Schultz, and D. Mattis. Two soluble models of an antiferromagnetic chain. *Annals of Physics*, 16(3):407–466, 1961.
- [4] P. Mazur and T.J. Siskens. Time correlation functions in the a-cyclic xy model. i. *Physica*, 69(1):259–272, 1973.
- [5] T.J. Siskens and P. Mazur. Time-correlation functions in the a-cyclic xy model. ii. *Physica*, 71(3):560–578, 1974.
- [6] E. B. Fel’dman, R. Bruschweiler, and R. R. Ernst. From regular to erratic quantum dynamics in long spin 1/2 chains with an xy hamiltonian. *Chemical physics letters*, 294(4-5):297–304, 1998.
- [7] E. B. Fel’dman and M. G. Rudavets. Regular and erratic quantum dynamics in spin 1/2 rings with an xy hamiltonian. *Chemical physics letters*, 311(6):453–458, 1999.
- [8] R. Bruschweiler and R. R. Ernst. Non-ergodic quasi-equilibria in short linear spin 1/2 chains. *Chemical physics letters*, 264(3-4):393–397, 1997.
- [9] J. Mossel and J.-S. Caux. Relaxation dynamics in the gapped XXZ spin-1/2 chain. *New Journal of Physics*, 12(5):055028–+, May 2010.
- [10] O. Lychkovskiy. Entanglement, decoherence and thermal relaxation in exactly solvable models. In *Journal of Physics: Conference Series*, volume 306, page 012028. IOP Publishing, 2011.
- [11] Z. Zhu, A. Aharony, O. Entin-Wohlman, and P. C. E. Stamp. Pure phase decoherence in a ring geometry. *Phys. Rev. A*, 81:062127, Jun 2010.
- [12] T. Niemeijer. Some exact calculations on a chain of spins. *Physica*, 36(3):377–419, 1967.
- [13] E.H. Lieb and D.W. Robinson. The finite group velocity of quantum spin systems. *Communications in Mathematical Physics*, 28(3):251–257, 1972.
- [14] L. Banchi, T. J. G. Apollaro, A. Cuccoli, R. Vaia, and P. Verrucchi. Optimal dynamics for quantum-state and entanglement transfer through homogeneous quantum systems. *Phys. Rev. A*, 82:052321, Nov 2010.
- [15] Abolfazl Bayat, Leonardo Banchi, Sougato Bose, and Paola Verrucchi. Initializing an unmodulated spin chain to operate as a high-quality quantum data bus. *Phys. Rev. A*, 83:062328, Jun 2011.

- [16] F. Haake. *Quantum signatures of chaos*, volume 54. Springer Verlag, 2010.
- [17] M. Feigenbaum. Universal behavior in nonlinear systems. *Los Alamos Science*, 1(1):4, 1980.
- [18] A. Peres. *Quantum theory: concepts and methods*, volume 57. Kluwer Academic Publishers, 1993.